

DRAFT - submitted to AJ

LUMINOSITIES AND PULSATONAL PROPERTIES OF RR LYRAE VARIABLES IN THE BAR OF THE LARGE MAGELLANIC CLOUD ¹

Gisella Clementini², Raffaele Gratton³, Angela Bragaglia²,

Eugenio Carretta³ and Luca Di Fabrizio²

²*Osservatorio Astronomico di Bologna, Via Ranzani 1, 40127 Bologna, ITALY*

³*Osservatorio Astronomico di Padova, Vicolo dell'Osservatorio 5, 35122 Padova, ITALY*

gisella@bo.astro.it, gratton@pd.astro.it, angela@bo.astro.it,
carretta@pd.astro.it, and lau@sean.bo.astro.it

ABSTRACT

New B,V CCD photometry in the standard Johnson system is presented for two $13' \times 13'$ fields (later referred to as "field A" and "field B") located close to the bar of the LMC and partially overlapping with fields #6 and #13 of the MACHO microlensing experiment. We detected 128 RR Lyrae variables in the two areas and obtained full coverage of the B and V light curves for 93 and 107 variables, respectively, among which 9 double-mode pulsators (RRd's). The average apparent luminosity of the single-mode RR Lyrae's with complete V and B light curves is $\langle V(\text{RR}) \rangle = 19.352 \pm 0.023$ (52 stars) and $\langle B(\text{RR}) \rangle = 19.762 \pm 0.023$ (48 stars) in field A, and $\langle V(\text{RR}) \rangle = 19.314 \pm 0.025$ (41 stars) and $\langle B(\text{RR}) \rangle = 19.656 \pm 0.030$ in field B (33 stars). The average apparent luminosity of the clump stars in the same fields is ~ 0.12 mag **brighter** than the RR Lyrae level ($\langle V_{\text{clump}} \rangle = 19.223 \pm 0.003$ and 19.200 ± 0.003 , in field A (5345 stars) and B (3639 stars), respectively). An estimate of the reddening within the two areas was obtained from the colors of the edges of the instability strip defined by the RR Lyrae variables. These values : $E(B-V) = 0.08 \pm 0.02$, and 0.06 ± 0.02 mag in field A and B, respectively, are in extremely good agreement with reddening values derived from Cepheids falling within 2 degrees from our fields ($E(B-V) = 0.07$ mag), and provide evidence for a small differential reddening existing between the two areas. When coupled with the apparent luminosities of the RR Lyrae's defined by the present photometry and the absolute magnitude derived from the Baade-Wesselink and the statistical parallaxes methods ($M_V(\text{RR}) = 0.68$ and 0.76 mag at $[\text{Fe}/\text{H}] = -1.5$, both methods known to favour the *short* distance scale) the new reddening estimates lead to distance moduli for the LMC of $\mu_{\text{LMC}} = 18.44 \pm 0.15$ and $\mu_{\text{LMC}} = 18.36 \pm 0.12$. On the other hand, the present determination of the V luminosity of the clump stars when combined with OGLE-II $\langle V - I \rangle = 0.89$ mag for the clump, and corrected back to our new reddening values

leads to $\langle I \rangle_0 = 18.10 \pm 0.07$ mag and moves the clump distance modulus of the LMC to 18.40 ± 0.07 and 18.44 ± 0.07 mag, whether Udalski (2000, ApJ, 531, L25) or Popowski (2000, AJ, 106, 703) metallicity-I luminosity relations for the clump stars are adopted.

All these values are only 1σ shorter than provided by the Population I distance indicators (e.g. the Cepheids), and allow to **reconcile** the *short* and *long* distance scale on a common value for the distance modulus of the LMC of $\mu_{\text{LMC}} = 18.50 \pm 0.07$.

Subject headings: distance scale – Magellanic Clouds – stars: oscillations – stars: variables: other (RR Lyrae) – techniques: photometry

1. Introduction

The Large Magellanic Cloud (LMC) is widely considered a benchmark in the definition of the astronomical distance scale, however no general consensus has been reached so far on its actual distance since a dichotomy at a 0.2-0.3 mag level seems to persist between *short* and *long* distance to the LMC as derived from Population I and Population II distance indicators. The state-of-art on the distance modulus of the Large Magellanic Cloud (LMC), as derived from various techniques and in the light of the recent astrometric results obtained with the accomplishment of the Hipparcos mission is displayed in panel (a) of Figure 1 where different symbols are adopted for Population I and II indicators. Figure 1a shows that, with a few exceptions (the red clump and the eclipsing binaries method, but see Section 7), the Population I distance indicators have a preference to cluster around a *long* distance modulus for the LMC in the range of 18.5–18.7 mag. An internal dichotomy is presented instead by the Population II indicators with a preference of the indicators based on "field stars" (Baade-Wesselink, B-W, and Statistical Parallax methods, in particular) to yield a *short* distance modulus of 18.3, while indicators based on "cluster stars", as for instance the Main Sequence Fitting method (Gratton et al. 1997, Carretta et al. 2000b) and the globular clusters dynamical models, or the pulsational properties of RR Lyrae's in globular clusters (Sandage 1993) seem to support a much *longer* modulus in the range 18.4-18.6. Indeed, the well-known discrepancy between *short* and *long* distance scales derived from old, Population II stars is still an unsolved issue (see e.g. Gratton et al. 1997), in spite of the impressive improvements in measuring distances achieved thanks to the Hipparcos mission. The average difference between the two scales (0.25-0.30 mag) translates into a difference of about $3\text{--}4 \times 10^9$ years in the corresponding age of the Galactic globular clusters and in turn in the age of the Universe.

The distance to the LMC from Population II objects is finally founded on the luminosity of the RR Lyrae variables: observations provide the "apparent luminosity" of the LMC RR Lyrae's $m(\text{RR}_{\text{LMC}})$, the various techniques provide the absolute luminosity of the RR Lyrae's $M(\text{RR})$, and

¹Based on data obtained at the 1.5 m Danish and 3.6 m ESO telescopes in La Silla- Chile

distance to the LMC simply follows from the well known relation between apparent and absolute magnitude. Two major estimates of the apparent luminosity of RR Lyrae variables in the LMC existed so far: Walker (1992a) published average luminosities for RR Lyrae’s in 7 clusters of the LMC; the mean dereddened apparent magnitude of the cluster RR Lyrae’s in his sample is 18.94 ± 0.04 mag (182 variables) at an average metal abundance of $[\text{Fe}/\text{H}] = -1.9$ and for an average reddening value of $\langle E(B - V) \rangle = 0.09$ mag (but with individual reddening values in the range $0.03 < E(B - V) < 0.18$ mag). More recently, the MACHO microlensing experiment has led to the discovery of about 8,000 RR Lyrae’s in the bar of the LMC (Alcock et al. 1996, hereinafter referred to as A96). The average dereddened apparent magnitude from a subsample of 500 of these variables is 19.09 at $[\text{Fe}/\text{H}] = -1.7$ (from A96 spectroscopic abundances for 15 RR Lyrae’s in their sample) and for an assumed reddening value of $E(B - V) = 0.10$ mag, according to Bessel (1991).

Estimates for the absolute magnitude of the RR Lyrae stars come from the B-W method (Liu & Janes 1990; Jones et al. 1992; Cacciari, Clementini & Fernley 1992; Skillen et al. 1993; Fernley 1994) and from the Hipparcos based Statistical parallaxes (Fernley et al. 1998a; Tsujimoto et al. 1998; Gould & Popowski 1998), applied to field RR Lyrae’s. Fernley et al. (1998b) provide a summary of previous B-W analyses and discuss the slope and zero-point of the RR Lyrae absolute magnitude – metallicity relation. They quote a zero point of $M_V(\text{RR}) = 0.98 \pm 0.15$ mag (at $[\text{Fe}/\text{H}] = 0.0$), and a mild slope of 0.18 ± 0.03 mag, given by the weighted average of the B-W slope (0.20 ± 0.04) and of results for 8 globular clusters (GCs) in M31 observed with the Hubble Space Telescope (Fusi Pecci et al. 1996: 0.13 ± 0.07). However, preliminary results based on an enlarged sample of 14 M31 GCs (Corsi et al. 2000) now seem to suggest a steeper slope of 0.21 mag/dex.

Statistical parallaxes lead to $M_V(\text{RR}) = 0.77 \pm 0.15$ mag at $[\text{Fe}/\text{H}] = -1.53$, 0.69 ± 0.10 mag at $[\text{Fe}/\text{H}] = -1.58$, and 0.77 ± 0.13 at $[\text{Fe}/\text{H}] = -1.60$, in Fernley et al. (1998a), Tsujimoto et al. (1998), and Gould & Popowski (1998) analyses, respectively, but do not provide information on the slope of the $M_V(\text{RR})$ - $[\text{Fe}/\text{H}]$ relation.

In the following we assume a value of $\Delta M_V(\text{RR})/\Delta[\text{Fe}/\text{H}] = 0.2$ mag/dex (which is supported by both the B-W and the new M31 results) to transform the above $M_V(\text{RR})$ values to the average metallicity of the LMC, assumed to be $[\text{Fe}/\text{H}] = -1.5$ (this is the most commonly adopted value for the LMC, and it was recently confirmed by the ΔS metal abundances derived by Bragaglia et al. 2000, for 6 RRd’s in the bar of the LMC) and derive $M_V(\text{RR}) = 0.72 \pm 0.15$ mag as average of the B-W (0.68 mag at $[\text{Fe}/\text{H}] = -1.5$)² and of the statistical parallaxes results (0.76 at $[\text{Fe}/\text{H}] = -1.5$). This value, when combined with Walker’s apparent luminosity for the LMC cluster RR Lyrae’s,

²The B-W determination of the absolute luminosity of the Galactic field RR Lyrae’s is being revised in order to test the effects on this technique of the most recent model atmospheres (Kurucz 1995; Castelli 1999; Canuto & Mazzitelli 1992) with various approximations in the treatment of convection, different values of turbulent velocity and more complete and accurate opacity tables, as well as the use of instantaneous gravity along the pulsation cycle. Preliminary results (Cacciari et al. 2000) give for one star at $[\text{Fe}/\text{H}] = -1.5$ (RR Cet) $M_V(\text{RR}) = 0.56$ mag, which is about 0.12 mag brighter than found from previous studies (e.g. Fernley et al. 1998b). The analysis is presently being performed on a larger sample of field RR Lyrae’s at $[\text{Fe}/\text{H}] = -1.5$ (Cacciari, Clementini & Castelli 2000).

leads to a distance modulus for the LMC of $\mu_{\text{LMC}}=18.30$ (at $[\text{Fe}/\text{H}]=-1.5$ dex) in agreement with the *short* distance scale. On the other hand, MACHO's value leads to a *longer* modulus of 18.39 mag for the LMC, but further complicates the scenario since it also seems to suggest that an intrinsic difference of ~ 0.1 mag might actually exist between field and cluster RR Lyrae's. In fact, if allowance is given for the 0.2 dex difference in metallicity between Walker's and A96 samples and according to $\Delta M_V(\text{RR})/\Delta[\text{Fe}/\text{H}]=0.2$, A96 apparent luminosity for the field RR Lyrae's is 0.11 mag *fainter* than Walker's apparent luminosity for the cluster variables.³

That an intrinsic difference at a $\sim 0.1 - 0.2$ mag level might actually exist between the luminosity of HB stars in globular clusters and in the field was suggested by Gratton (1998) calibration of absolute magnitude of field horizontal branch (HB) metal-poor stars with good parallaxes from Hipparcos. Furthermore, the latest evolutionary models by Sweigart (1997), which include some extra-mixing of He and other heavy elements (C,N,O), give some more support to this hypothesis, since there is observational evidence for extra-mixing in cluster red giants but not among field stars (Gratton et al. 2000). However, this suggestion was tested qualitatively by Catelan (1998) and, more recently and in a more quantitative way, by Carretta, Gratton & Clementini (2000a) using the pulsational properties of a selected sample of field and cluster RR Lyrae's. Their results show that field and cluster variables, in our Galaxy, cannot be distinguished in the $\Delta \log P_{\text{field-cluster}} - [\text{Fe}/\text{H}]$ plane, so that the actual existence of a luminosity difference between field and cluster variables seems unlikely.

A further estimate of the apparent dereddened average luminosity of the RR Lyrae's in the LMC was obtained by Udalski (1998a): $\langle V_0(\text{RR}) \rangle = 18.86 \pm 0.04$ mag at an average metallicity of $[\text{Fe}/\text{H}]=-1.6$ and for assumed reddening values of $E(B-V)=0.14, 0.16$ mag [transformed from Udalski's (1998a) $E(V-I)=0.22, 0.26$ mag according to Cardelli et al. (1989) relation between $E(B-V)$ and $E(V-I)$], based on 104 RR Lyrae's observed in the second phase of the Optical Gravitational Lensing Experiment, OGLE-II (Udalski, Kubiak & Szymański 1997). This value has been lately revised to $\langle V_0(\text{RR}) \rangle = 18.94 \pm 0.04$ mag (Udalski et al. 1999), on the claim that extinction was slightly overestimated in Udalski (1998a). Udalski et al. (1999) conclude that the revised estimate is "in very good agreement" with the mean brightness of Walker (1992a) cluster RR Lyrae's in the LMC. However, if the 0.3 dex difference in metallicity between Udalski (1998a) and Walker (1992a) samples is taken into account, Udalski et al. (1999) dereddened average luminosity is in fact 0.06 mag *brighter* than Walker's.

On the other hand, explanations other than intrinsic differences between field and cluster RR Lyrae's are possible for the differences in the apparent luminosity of the LMC RR Lyrae's found by Walker (1992a), A96 and Udalski et al. (1999):

- (i) MACHO photometry is in nonstandard blue and red passbands which are very different

³Even with the steep slope of $\Delta M_V(\text{RR})/\Delta[\text{Fe}/\text{H}]\sim 0.3$, supported by Sandage (1993) there is a 0.09 mag difference between Walker's and A96 mean apparent luminosities for the RR Lyrae's.

from the Johnson photometric passbands of Walker’s cluster RR Lyrae photometry (see fig. 1 of Alcock et al. 1999; hereinafter referred to as A99). Additional concern also arises from the accuracy of the MACHO photometry at the limiting magnitude typical for the LMC RR Lyrae’s (19-20 mag). This problem is clearly shown in fig. 6 of A99. Udalski et al. (1997) provide a detailed description of the instrumental set up of OGLE-II. They briefly mention the OGLE-II filter passbands and comment that except for the ultraviolet filter, they are very close to the standard system;

(ii) it may be possible that due to projection effects combined to small number statistics, the LMC globular clusters in Walker (1992a) sample are, on average, closer to us than the bar of the LMC. Indeed, Walker (1992a) assumed that his clusters were on the same plane as younger populations, based on similarity in kinematics (Schommer et al. 1992). However, this assumption may be questioned in view of the large scatter of the individual objects in the sky (see Figure 2) and Walker himself cautions that at least one of the clusters in his sample (NGC 1841) could actually be about 0.2 mag closer to us;

(iii) finally, a major crucial point is the actual reddening of the LMC. Walker (1992a; see his tab. 1) derives reddening values from the colors of the instability strip edges defined by RR Lyrae’s in each cluster of his sample. These reddenings range from $E(B-V) = 0.03$ for the Reticulum cluster, to $E(B-V) = 0.18$ for NGC 1841, with an average value of $E(B-V) = 0.09$ mag. However, in some cases with the adoption of such reddening values the dereddened instability strip of some clusters appears too blue (NGC 1835); in others it may be not totally filled (NGC 1786, NGC 1841). Reddening estimates are rather uncertain in these cases. In turn, the average value of 0.09 mag could well be an overestimate of the actual reddening. A96 do not derive an independent reddening estimate, but simply assume $E(B-V) = 0.10$, following Bessell (1991). This is the most commonly adopted value for the reddening of the LMC found in the literature. Udalski (1998a) adopts an average reddening value of $E(B-V) = 0.15$ mag (transformed from $E(V-I) = 0.24$ mag, see above discussion) for his RR Lyrae’s sample, but Udalski et al. (1999) claim that this value is too high. They do not give the revised value, but extrapolating back from their revised value of $\langle V_0(RR) \rangle = 18.94$, we argue that the new $E(B-V)$ should be of 0.12 mag. The 0.03 mag difference between Walker (1992a) and Udalski et al. (1999) reddenings largely accounts for the difference existing between their dereddened average luminosities of the LMC RR Lyrae’s, once the difference in the metallicity of the two samples is taken into account. On the other hand, it is possible that Udalski et al. (1999) reddening value is not too much overestimated, since OGLE-II LMC fields where RR Lyrae’s were extracted from are definitely more centered on the LMC bar than our field A for which we estimate a reddening of 0.08 mag. In this case, systematic differences between OGLE-II and Walker (1992a) Johnson photometric systems (with OGLE-II V being systematically brighter by ~ 0.06 mag than Johnson V), could explain the difference existing between Udalski et al. (1999) and Walker (1992a) dereddened average luminosities for the RR Lyrae’s.

Finally, we recall that the reddening value derived from Cepheids in the bar of the LMC is $E(B-V) = 0.07$ mag (Laney & Stobie 1994), i.e. ~ 0.02 - 0.03 mag smaller than Walker’s and A96, and about 0.05 mag smaller than Udalski et al. (1999).

We have undertaken an observational campaign with the purpose of obtaining new accurate B, V photometry directly tied to the Johnson photometric system for a large sample of RR Lyrae variables in the bar of the LMC, as well as to acquire low resolution spectra for some of the LMC double-mode pulsators discovered by Alcock et al. (1997, hereinafter referred to as A97). The original purposes of the observing program were the definition of the average luminosity and the investigation of the mass-metallicity relation defined by the RR Lyrae’s in the bar of the LMC, to be compared with that obtained for the Galactic globular clusters, in order to see whether an intrinsic difference in luminosity, possibly due to a difference in mass, might exist between field and cluster RR Lyrae’s, which could be responsible for the well-known dichotomy between *short* and *long* distance scales.

The new photometric data have allowed us to define a very precise average apparent luminosity for RR Lyrae variables in the bar of the LMC, which can be compared to Walker (1992a) estimate for the cluster RR Lyrae’s, as well as an accurate estimate of the mean apparent luminosity of the LMC clump stars found in the same fields. These data also allow an independent estimate of the reddening along the bar of the LMC from the colors of the edges of the instability strip defined by the LMC bar RR Lyrae’s. Metal abundances were derived from the spectra of 6 stars using the ΔS method (Preston, 1959). We found metallicities in the range of -1.09 to -1.78 , with mean metallicity -1.5 ; the spectroscopic results are described in a separate paper (Bragaglia et al. 2000).

We discuss here the photometric data, which are presented in Section 2. The period search procedure is described in Section 3. The apparent luminosity and the pulsational properties of single and double-mode RR Lyrae variables in our sample are discussed in Section 4 and 5, respectively. Section 6 addresses the problem of the actual reddening of the LMC, and new estimates of $E(B-V)$ from the color of the edges of the instability strip defined by our RR Lyrae sample are presented. In Section 7 we analyse the apparent magnitude and the luminosity distribution of the clump stars in our observed fields. In Section 8 we compare our new estimate of the average luminosity of the RR Lyrae variables in the LMC to other photometric data available in the literature. Finally, in Section 9 we discuss the impact of the present new photometry on the derivation of the distance to the LMC.

2. Observations and reductions

2.1. Observed fields and observing strategy

The photometric observations were carried out at the 1.54m Danish telescope located in La Silla, Chile, on the nights 4 – 7 January 1999, UT. The telescope was equipped with the DFOSC focal reducer, mounting the CCD #C1W7, a Loral/Lesser 2052x2052 pixel chip, with scale 0.4 arcsec/pix, field of view of 13.7 arcmin², and a filter wheel mounting the Johnson standard system.

The MACHO collaboration (A96) discovered about 7,900 RR Lyrae’s in the $\sim 39,000$ arcmin²

of the LMC they surveyed, and published coordinates and differential curves for 73 RRd’s (A97). We observed at two different positions, later called A and B, almost centered on the bar of the LMC and contained in fields #6 and #13 of the MACHO microlensing experiment (see <http://www.macho.mcmaster.ca>). The observed fields and their positions with respect to MACHO’s map of the LMC are shown in Figure 3. These positions were chosen in order to maximize the number of known RRd (A97) observable with only two pointings: 5 and 4 in field A and B, respectively. Coordinates (epoch 2000) of the two centers are: $\alpha = 5:22:43.9$, $\delta = -70:34:15$ (field A), and $\alpha = 5:17:27.9$, $\delta = -71:00:14$ (field B). Observations were done in the Johnson-Bessel B and V filters (ESO 450, and ESO 451), and we obtained 58 V and 27 B frames for field A, and 55 V and 24 B frames for field B. Seeing conditions varied during each night and in the whole observing run; typical values were in the range 1.2-1.8 arcsec. Exposure times varied from 180^s to 300^s in V and from 360^s to 480^s in B, depending on weather-seeing conditions and hour angle. They were chosen as an optimal compromise between S/N and time resolution of the light variation of the RR Lyrae variables. Eighteen stars from Landolt (1992) standard fields were observed during each night in order to secure the transformation to the standard Johnson photometric system.

After debiasing and correcting for flat field, a preliminary data reduction was first performed using SExtractor (Bertin & Arnouts 1996), which admittedly is not the best choice for point sources in crowded fields, since it works with aperture photometry, but was precise enough to identify a large number of variables falling into the two fields and to build preliminary light curves for all 9 RRd’s known from A97. Epochs of maximum light of the RRd’s determined by the present photometry were used, together with periods from A97, to define the time of minimum light and properly schedule the following spectroscopic observations. Spectra for 7 of the 9 RRd variables (along with calibration objects) were obtained with EFOSC2 at the 3.6 m ESO telescope during the nights 17-18 January 1999. A detailed description of the spectroscopic dataset and analysis can be found in Bragaglia et al. (2000).

2.2. Reductions

Final reduction and analysis of the photometric data was done using the package DoPHOT (Schechter, Mateo & Saha 1993) which uses an elliptical Gaussian PSF to evaluate instrumental magnitudes. We used a variable PSF, and run DoPHOT independently on all frames, with a threshold for source detection of 5σ above the local sky. Using a private software written by P. Montegriffo, the resulting tables were then aligned to the ”best” frame for each field (i.e., to the one taken in better seeing and weather conditions, and near meridian) and stars were counteridentified. Catalogues were produced, all containing the same number of stars, and with a unique identifying number: this helped in the following variability search and study. The number of objects classified as stars in each frame is variable (several thousands to about 30,000). The final catalogues, after counteridentification in V and B contain about 29,000 objects for field A and about 23,000 for field B, which is reasonable since field A is slightly closer to the LMC bar and thus more crowded than

field B.

Aperture corrections were derived for the "master frames", i.e. for the best B and V frames in each field, the same used for the absolute photometric calibration. We chose about 10 bright and relatively isolated stars in each frame, and further cleaned them from companions, usually very faint in comparison, up to a radius of 20-25 pixels (note that the aperture used to compute the star magnitude has a radius of 12-13 pixels). We used the task *imedit* in Iraf⁴, and substituted the objects with the local average sky value. Aperture magnitudes for these stars were computed using *phot* in Iraf, the same task used for the photometric standards, and the derived mean difference between PSF and aperture magnitudes was used to correct the PSF magnitudes of all other objects. The aperture corrections (aperture minus PSF), based on a zero point of 30 in the *phot* task, were 30.04 and 30.06 for the V filter, and 30.03 and 30.04 for the B filter, with scatter around the mean value of 0.02-0.04 mag.

2.3. Night extinction calculation and absolute calibration

Of the four nights, only one was tainted by cirri, while the three others were of photometric quality, especially the third one (January 6 1999), which we used for the absolute photometric calibration. The extinction coefficients for this night were computed directly from our fields. 13 and 12 well isolated and stable stars were chosen within fields A and B respectively; we used 18 and 9 V measures at varying airmass ($1.322 < \sec z < 1.869$), and 10 and 3 B measures ($1.323 < \sec z < 1.906$) to derive the following first order extinction coefficients: $K_V = 0.114 \pm 0.002$ ($\sigma=0.011$ - 25 stars) and $K_B = 0.252 \pm 0.006$ ($\sigma=0.029$ - 25 stars). They well compare with the standard average values of the site (~ 0.12 and 0.22 in V and B, respectively).

To secure the transformation to the standard Johnson photometric system, we observed the Landolt (1992) standard star fields PG0231+051 and SA95 at the beginning of the night, and PG0918+029 at the end. These fields contain a total of 18 standards, completely covering the color range of interest; they have magnitude $12.064 < V < 16.275$ and color $-0.329 < B - V < 1.457$. The derived calibration equations are:

$$V = 1.00(\pm 0.02) \times v - 5.69$$

$$V - v = 0.001(\pm 0.014) \times (b - v) - 5.719$$

$$B - b = 0.096(\pm 0.012) \times (b - v) - 6.005$$

where B, V are in the Johnson system, while b , v are the instrumental magnitudes. The calibration equations are shown in Figure 4. Departure from linearity and the color term in V are very small and were further neglected. Photometric zero points are of 0.02 mag both in V and B.

⁴Iraf is distributed by the National Optical Astronomical Observatories, which is operated by the Association of Universities for Research in Astronomy, Inc., under cooperative agreement with the National Science Foundation.

Calibrated color-magnitude diagrams of field A and B are shown in Figure 5 and Figure 6; they contain 22,925 and 19,005 objects, respectively. Both diagrams show a prominent red clump population. We will discuss this point at some length in Section 7.

3. Identification of the variables and period search

Variables stars were identified using the program VARFIND, by P. Montegriffo, written for this purpose. The program normalizes the files containing measures of the fitted stars to a reference file, then computes the average magnitude of each star and its sigma. Candidate variable objects were picked up thanks to their large sigmas. Each candidate object was then checked for variability using the program GRATIS (GRaphical Analyzer TIme Series) a code being developed at the Bologna Observatory which is directly interfaced to VARFIND, and allows to display the sequence of differential measurements of the object with respect to a selected reference stable star as a function of the Heliocentric Julian day of observation, and to perform a period search on its data (see below). Figure 7 shows the typical sigma *vs* magnitude plot used to identify variables in the V frames of field A: crosses mark the actually variable objects identified in this field (93 stars). The region defined by the RR Lyrae variables is clearly visible at $18.6 < V < 19.8$ mag, while variables around $15.1 < V < 16.6$ mag are Cepheids.

Variables were searched for in the V and B frames independently, and the search procedure was repeated several times, subsequently lowering the detection threshold. A total number of 1165 and 747 objects were checked for variability in field A and B, respectively. We are confident that our identification of the RR Lyrae’s is complete as far as the R Rab variables are concerned while, giving the smaller amplitudes and the crowding conditions of the observed fields (field A in particular), we cannot totally rule out that some RRc’s may have escaped detection.

As an alternative approach we detected the variables using the following procedure :

- (i) we selected all stars in a 1.5 magnitude bin bracketing the expected range for RR Lyrae variables on a reference V frame;
- (ii) we determined the mean frame-to-frame offset with respect to the reference frame by iteratively eliminating all stars deviating more than 2.5σ from the average. These mean offsets are finally based on about 2500 ”constant” stars having a V magnitude similar to that of the RR Lyrae’s;
- (iii) we then determined the average V magnitude and its *rms* for all stars by combining all V frames, using the offsets determined in step (ii);
- (iv) all stars with *rms* larger than three times the typical value for this magnitude range (again determined iteratively) were examined closely for variability looking for possible periods in the range 0.2-1 day;
- (v) the same procedure was repeated using the B frames.

On the whole, results obtained using the two procedures agree very well.

According to A96 average density of RR Lyrae’s in the LMC, we expected about 40 RR Lyrae’s in each of our fields. We actually detected 152 variable objects in the two fields, and an additional 10 candidates. 128 of the certain variables are of RR Lyrae type (118 single-mode and 10 double-mode RR Lyrae’s, one of which not previously known from A97; see Sections 4 and 5), corresponding to a density 60% larger than the expected LMC RR Lyrae average density. The number of variables detected in the two fields whose type could be unambiguously assigned is given in Table 1 where variables are divided by type and field. All variables were studied using their differential photometry with respect to a number of stable, well isolated objects used as reference stars. These were some of the stars used to compute the night extinction and the aperture corrections. Coordinates and calibrated magnitudes of the reference stars are given in Table 2 along with the number of measures of each stars. Periods for all the identified variables were defined using the program GRATIS run on the differential photometry. GRATIS performs a period search according to two different algorithms : (a) a Lomb periodogram (Lomb 1976, Scargle 1982) and (b) a best-fit of the data with a truncated Fourier series (Barning 1962). The adopted period search procedure was first to perform the Lomb analysis on a wide period interval. Then the Fourier algorithm was used to refine the period definition and to find the best fitting model from which to measure the amplitude and the average luminosity of each variable. The period search employed each of the complete B and V data-sets. Periods and epochs were derived for all the 152 variables, accurate to the third or fourth digit, depending on the light curve data sampling, which, in the best cases is 58 V and 27 B data points for the variables in field A, and 55 V and 24 B data points for the variables in field B.

GRATIS also performs a search for multiple periodicities, and was run on the data of the 10 double-mode variables falling in our two fields, 9 in A97 and 1 newly discovered. However, our data sampling for these stars is too poor to allow a very accurate derivation of the double-mode periodicities. Out of the 152 variables identified in the two fields we have full coverage of the V and B light curves for 99 and 83 RR Lyrae’s, respectively. We also fully covered the light curve (particularly in V) of 8 eclipsing binaries with short orbital period ($P < 0.48$), while Cepheids are poorly sampled in our photometry, due to their longer periods. Examples of the light curves of an *ab*, a *c* and *d* type RR Lyrae, as well as of an eclipsing binary in our sample are shown in Figure 8 and Figure 9. The full catalogue of the light curves is published in Di Fabrizio et al. (2000). Average residuals from the best fitting models for RR Lyrae’s with well sampled light curves are 0.02-0.03 mag in V and 0.035-0.06 mag in B for the single-mode variables, and 0.05-0.13 in V and 0.07-0.13 in B for the double-mode variables. The lower accuracy of the B light curves is caused by the larger intrinsic faintness of the RR Lyrae variables in this passband and the worse sampling.

4. Luminosities and pulsational properties of the single-mode RR Lyrae's

4.1. The apparent luminosity

Best fitting models of the V and B light variations were computed for all variables with full light curve coverage, using GRATIS. These are Fourier series with the number of harmonics generally varying from 1 to 4 for the *c*-type RR Lyrae's, and from 4 to 10 for the *ab*-type variables (for details, see Di Fabrizio et al. 2000). Models were further hand-edited whenever needed. This actually occurred only in a few cases and mainly for the *ab*-type variables, when the skewness of the light curves could be reproduced with difficulty, and only using a large number of harmonics and at the cost of disturbing unphysical oscillations of the model in other portions of the curve. Intensity average $\langle V \rangle$ and $\langle B \rangle$ magnitudes, as the integral over the entire pulsation cycle of the models best fitting the observed data, were derived for all the variables with complete light curves. Figure 10 shows the Number *vs* $\langle V \rangle$ histogram of the single-mode RR Lyrae's in our sample. The average apparent luminosities of the single-mode Lyrae's with full coverage of the V and B light curves is: $\langle V \rangle = 19.352 \pm 0.023$ ($\sigma=0.162$, 52 stars), $\langle B \rangle = 19.762 \pm 0.023$ ($\sigma=0.163$, 48 stars) in field A; and $\langle V \rangle = 19.314 \pm 0.025$ ($\sigma=0.161$, 41 stars), $\langle B \rangle = 19.656 \pm 0.030$ ($\sigma=0.174$, 33 stars) in field B.

There is a difference of 0.04 and 0.10 mag, respectively, between the average V and B magnitudes of the RR Lyrae's in the two fields. These differences are explained by a difference in the reddening affecting the two areas (with field A being about 0.02 mag more reddened than field B), as derived from the colors of the edges of instability strip defined by the RR Lyrae variables in our sample (see Section 6). A few RR Lyrae's were discarded when calculating these average values. These were foreground objects (2 RRc and 1 RRab in field A and B, respectively) and stars severely affected by blending (2 objects in field A) or variables whose light curves are suspected to be not evenly covered (5 and 1 objects in V, and 9 and 8 in B, for field A and B, respectively).

The intrinsic dispersion of the average B and V apparent luminosities (and, in turn, of the average B and V absolute magnitudes) of the RR Lyrae's in the two fields is: $\sigma_B \sim 0.17$ and $\sigma_V \sim 0.16$ mag, respectively. A number of sources contribute to form these dispersions, they are (i) the photometric errors of the present photometry: 0.03 mag; (ii) the metallicity distribution of the RR Lyrae in our sample. The metallicity distribution of the 6 RRd's in field A and B analyzed by Bragaglia et al. (2000) have a 1σ dispersion of 0.28 dex around the mean value of $[\text{Fe}/\text{H}] = -1.5$; this corresponds to a magnitude dispersion of 0.06 mag (according to $\Delta M_V(\text{RR})/\Delta[\text{Fe}/\text{H}] = 0.2$ mag/dex). While the metallicity range spanned by these 6 RRd's is likely to be an underestimate of the actual metallicity range existing between the total sample of RR Lyrae's in these areas of the LMC, their metallicity dispersion well compares with the ~ 0.4 dex dispersion we would derive taking into account the total period distribution spanned by the *ab* type RR Lyrae's in our sample ($0.^d35$ – $0.^d74$). On the whole we think that 0.06–0.08 mag is a proper estimate for the magnitude dispersion due to the metallicity distribution of the RR Lyrae's in our sample; (iii) the level of evolution off the Zero Age Horizontal Branch (ZAHB) of the variables in our sample. Here what

matters is not the global systematic difference between ZAHB and average luminosity of the RR Lyrae's, but rather the dispersion around the average RR Lyrae luminosity due to the evolution off the ZAHB of each individual RR Lyrae. Sandage (1990) studied the vertical height of the horizontal branch of a number of globular clusters of different metallicity, and found for M3 and NGC 6981, clusters which metallicity is close to the average value of the LMC, horizontal branch luminosities with standard dispersions of 0.064 and 0.097 mag respectively, giving an average value of 0.08 mag⁵; and, finally (iv) the intrinsic depth of the observed fields. Adding up in quadrature the dispersion contributions due to photometric errors, metallicity distribution and evolution off the ZAHB we obtain a total dispersion of 0.09–0.13 mag to compare with the observed V dispersion of 0.16 mag. This gives us some hint on the actual intrinsic depth of our observed fields for which we derive an upper limit of about 0.10 mag corresponding to a dispersion in depth of 5% or 2.5 kpc (for an assumed distance modulus $\mu_{\text{LMC}}=18.50$ mag, see Section 9).

The comparison of the apparent luminosity of our RR Lyrae sample with other estimates available in the literature (Walker 1992a; A96; and Udalski et al. 1999) is postponed to Section 8.

We have formed $\langle B \rangle - \langle V \rangle$ colors from the intensity average B and V magnitudes for all the variables with complete light curves. The intensity average magnitudes and colors ($\langle V \rangle$, $\langle B \rangle - \langle V \rangle$) were used to place the variables on the color-magnitude diagrams of the two fields, shown in Figure 5 and Figure 6. Finally, Figure 11 shows the comparison of the $\langle M_{V0} \rangle$ vs $(\langle B \rangle - \langle V \rangle)_0$ distributions of the RR Lyrae's in the LMC field A and B separately, with the instability strips defined by the variables in the globular clusters M3 (Carretta et al. 1998) and M15 (Bingham et al. 1984), whose edges are shown by the solid and dashed lines in Figure 11. In the comparison we have assumed $E(B-V)_{\text{LMC-fieldA}} = 0.08$ and $E(B-V)_{\text{LMC-fieldB}} = 0.06$ (see Section 6), $E(B-V)_{\text{M3}}=0.00$ (Ferraro et al. 1997) and $E(B-V)_{\text{M15}}=0.10$ (Bingham et al. 1984) and a standard value of $A_V=3.1 \times E(B-V)$ for the total visual absorption. Distance moduli were $(m_V - M_V)_{\text{LMC}}=18.54$ (Carretta et al. 2000b), $(m_V - M_V)_{\text{M3}}=14.94$ (Ferraro et al. 1997) and $(m_V - M_V)_{\text{M15}}=15.11$ (Djorgovski 1993).

RR Lyrae's in both field A and B are very well confined within the edges of the instability strip defined by the M3 variables thus showing the similarity of our LMC RR Lyrae sample more to variables in the Oosterhoff (1939) type I cluster M3, than to Oo-type II clusters like M15 (see Section 4.2) and giving support to our choice for the reddening value in the two areas (see Section 6).

⁵This is likely to be an overestimate of the real contribution due to evolution, because the field RR Lyrae population should be dominated by stars closer to the ZAHB than variables in clusters at same metallicity (see Carney et al. 1992)

4.2. The period distribution

Three of the 118 single-mode RR Lyrae’s in our sample are suspected to be foreground objects since their average apparent luminosity is about 0.7-1.0 mag brighter than for the other variables. The period distribution of the remaining 115 RR Lyrae’s is shown in Figure 12. Two peaks are clearly visible in the distribution, corresponding to the *c* (37 objects) and the *ab* (78 objects) type pulsators. The number of *c*-type pulsators divides almost equally among the two fields (19 and 18 RRc’s in field A and B, respectively). On the other hand, the number of RRab’s is about 50% larger in field A. This difference, although not statistically significant, may suggest that we could be missing some *c* type pulsators in field A.

The mean period of the *c* and *ab* type RR Lyrae’s is $\langle P_{RRc} \rangle = 0.^d321$ ($\sigma = 0.050$ – 37 stars) and $\langle P_{RRab} \rangle = 0.^d573$ ($\sigma = 0.074$ – 78 stars), respectively, to compare with $0.^d342$ and $0.^d583$ of A96. Our $\langle P_{RRab} \rangle$ is in very good agreement with the value of $0.^d568$ found by Kinman et al. (1991) from a compilation of the period distributions of 122 *ab*-type variables in 6 fields of the LMC (see tab. 7 and fig. 3 in that paper).

A96, on the basis of their $\langle P_{RRab} \rangle = 0.^d583$, conclude that the preferred period of the *ab*-type variables of the LMC falls between the periods of the Galactic RR Lyrae stars of OoI and OoII types, but it is actually closer to the Oo I cluster periods (being $\langle P_{RRab} \rangle = 0.^d55$, and $0.^d65$ in the Oo I and II clusters, respectively).

This finding is confirmed and reinforced by our results which also show that the average pulsational properties of the variables in the two separate fields are slightly different, with variables in field B being more definitely of Oo type I. Field B contains in fact a large number of *ab* type RR Lyrae with periods around half a day, as shown by the average periods computed keeping the variables in the two fields separate. These are: $\langle P_{RRc} \rangle = 0.^d314$ ($\sigma = 0.053$ – 19 stars), $\langle P_{RRab} \rangle = 0.^d588$ ($\sigma = 0.069$ – 48 stars), and $\langle P_{RRc} \rangle = 0.^d328$ ($\sigma = 0.047$ – 18 stars), $\langle P_{RRab} \rangle = 0.^d547$ ($\sigma = 0.077$ – 30 stars), in field A and B, respectively.

B and V amplitudes (A_B , A_V) were calculated for all the RR Lyrae’s with full coverage of the light curve as the difference between maximum and minimum of the best fitting models (see Di Fabrizio et al. 2000), and have been used together with the newly derived periods to build the period - amplitude diagrams shown in Figure 13. The overlap in the transition region between *ab* and *c* type is very small (3 objects, see Figure 12 and Figure 13) and the transition period between *c* and *ab* type occurs in our sample at $P_{tr} \sim 0.^d40$, while $P_{tr} = 0.^d457$, in A96.

Our shortest period *ab* type RR Lyrae’s are: star #4859 in field B, $P = 0.^d349$ and amplitudes $A_V = 1.05$ and $A_B = 1.17$ mag; star #19450 in field A, $P = 0.^d398$, $A_V = 1.34$ and $A_B = 1.67$ mag; star #2407 in field B, $P = 0.^d403$, $A_V = 0.40$ mag and $A_B = 0.51$ mag [this object has very asymmetric light curves which contrast with the rather small amplitudes of the light variation, if the star is a fundamental mode pulsator (see details in Di Fabrizio et al. 2000)]; and star #19037 in field B, $P = 0.^d411$, $A_V = 1.42$ and $A_B = 1.85$ mag. All these variables are labelled in the period-amplitude

distributions in Figure 13.

The observed light curves of #4859, #19450 and #19037 have been compared with theoretical light curve prescriptions based on Bono et al. (1977a,b) models for RR Lyrae variables, and confirmed to be variables of Bailey *ab* type. This comparison for the large amplitudes and very short period of #4859 also suggest that (i) this variable should be at the very blue edge of the fundamental mode of pulsation (where amplitudes for *ab* pulsators reach maximum values) and (ii) the star should have very high metal abundance: $[\text{Fe}/\text{H}] \sim -0.3, -0.5$ dex (M. Marconi 2000, private communication).

The shortest period *c* type is star #3216 in field A with $P=0.^d218$, $A_V=0.41$ mag and $A_B=0.53$ mag, while the longest period *c* type is #6415 in field A, with $P=0.^d442$, $A_V=0.43$ mag and $A_B=0.49$ mag.

A96 discuss at some length the existence in their period and amplitude distributions (see figs. 1 and 6 of A96) of an extra-large number of variables with period around $0.^d28$ day, which have asymmetric light curves, but low amplitudes. A96 classify these variables as possible second-overtone RR Lyrae's (type *e*). Figure 12 and Figure 13 do not show clear evidences for an extra peak around $P \sim 0.^d28$. However, we only have 7 objects in the period range from $0.^d269$ to $0.^d290$ (4 in field B and 3 in field A), and none of them shows anomalously asymmetric light curves (see Di Fabrizio et al. 2000). Two RRc's of slightly longer period have very asymmetric curves, these are: #10320: $P=0.^d291$, $A_V=0.26$ and $A_B=0.43$ in field A (this star is not included in Figure 13 since it was found to be a foreground object); and #7490: $P=0.^d305$, $A_V=0.44$ and $A_B=0.50$ in field B.

The $A_V - \log P$, $A_B - \log P$ distributions of the variables in the two fields are similar particularly in V, where we have a larger number of variables with full coverage of the light curve (see Figure 13), and resemble fig. 6 of A96 with two major differences: (i) owing to our data sampling (observations in 4 consecutive nights) we do not have full coverage of the light curve, hence we cannot derive A_V and A_B values, for variables with periods longer than $0.^d70$ ($\log P > -0.16$), and (ii) our A_V amplitudes range is slightly larger than in A96, with A_V values from 0.30 to 1.40 mag in our sample to compare with 0.35-1.35 in A96.

A96 draw the attention to (i) the large number of Bailey *b* type RR Lyrae with amplitude less than 1.0 mag in their period-amplitude distribution (these variables outnumber by a factor 2 those with visual amplitudes larger than 1.0 mag); and to (ii) the paucity of stars with V amplitude of 0.9 ± 0.05 mag in the period range $-0.3 < \log P < -0.2$. Field A shows some evidence for a lack of *ab* type variables with amplitudes in the range $0.85 < A_V < 0.90$ mag and $1.0 < A_B < 1.15$ mag, however the *a* and *b* variables seem to be equally distributed around this gap in agreement with Walker (1992b, 1992c) finding for the LMC globular cluster variables. On the other hand, the *ab* type variables in field B seem to be uniformly distributed in the amplitude range $0.60 < A_V < 1.20$ mag, with only very few objects (3 in total) overcoming these limits.

The period - amplitude distributions of the LMC variables were compared with the relations

defined by the *ab* type RR Lyrae’s in the globular clusters M3 and M15, shown by the solid lines of Figure 13, taken from Carretta et al. (1998) for M3 and Bingham et al. (1984) for M15. These were computed as follow: we first derived the period-amplitude relations using the M3 sample which is more extended; then we shifted the intercept of these relations while holding fixed the slopes, until a good fit (by eye) was obtained also for the variables in M15, which are too few in number to give a satisfactory best fit by themselves.

RR Lyrae’s in field B seem to better follow the amplitude-period relations of the variables in M3 and, as already noted in the first part of this section, to belong to the OoI type. Variables in field A, instead, have pulsational properties more intermediate between the two Ooostheroff types.

5. The double-mode pulsators in our sample

According to A97, nine double-mode pulsators were expected to fall in the observed areas. We actually detected all of them and also found evidence for one possible additional RRd candidate not previously known from A97 : star #2419. This variable is tentatively classified as *d*-type mainly because of the large scatter of the observed V light curve (0.08 mag) which has no obvious explanation since the object is rather faint but is not blended to other stars on the frames. We fully covered the light variation of all RRd’s in our sample, however our data sampling of their light curves is too coarse to allow a firm identification of the two double-mode periodicities, particularly for stars with fundamental periods around half a day. Periods from A97 have been adopted to phase the data of these variables apart from star #2419 for which we use our period determinations.

Intensity average $\langle B \rangle$ and $\langle V \rangle$ magnitudes of the 10 RRd’s are given in Table 3. For a comparison we also give the $\langle V \rangle$ values of A97 for these stars. Variables are identified by our number, by the number in Di Fabrizio et al. (2000) catalogue, and by A97 identifier preceded by two letters indicating the field the variable belongs to and an ordering number according to tab.1 of A97. The mean of the intensity average $\langle V \rangle$ and $\langle B \rangle$ values for the 9 RRd’s in common with A97 is $\langle V \rangle = 19.28 \pm 0.07$ ($\sigma = 0.21$ - 9 stars), and $\langle B \rangle = 19.66 \pm 0.08$ ($\sigma = 0.25$ - 9 stars), to compare with A97 $\langle V \rangle = 19.13 \pm 0.04$ ($\sigma = 0.111$ - 9 stars). The average difference in V (this paper — A97) is $\Delta V = 0.15 \pm 0.04$ ($\sigma = 0.13$ - 9 stars).

We have also made averages keeping the RRd variables of the two fields separate and find that while $\langle V \rangle$ and $\langle B \rangle$ values for the RRd’s in field A (19.34 ± 0.08 and 19.72 ± 0.09 , average on 6 stars) are in very good agreement with the average values derived from the single-mode pulsators in the same field (19.35 ± 0.02 and 19.76 ± 0.02 , respectively), RRd’s in field B are on average ~ 0.1 mag brighter (19.22 ± 0.10 and 19.56 ± 0.12 , average on 4 stars) than the single-mode variables in the same field (19.31 ± 0.03 and 19.66 ± 0.09 , respectively). A totally similar trend is found in A97 $\langle V \rangle$ values.

ΔS metal abundances have been derived for 6 of the RRd’s, they range from -1.09 to -1.78 in $[\text{Fe}/\text{H}]$; complete results of the spectroscopic analysis are described in Bragaglia et al. (2000).

6. The reddening of the LMC

The classical value of the reddening for the LMC bar is $E(B-V)=0.10$ (Bessel 1991).

The reddening maps (based on IRAS data) of Schlegel, Finkbeiner & Davis (1998) give upper limits of $E(B-V)=0.218$ and 0.128 for field A and B, respectively. The foreground reddening, measured from dust emission in an annulus surrounding the LMC, is $E(B-V)=0.075$. From these, we may estimate median reddening values of $E(B-V)=0.146$ and 0.102 for field A and B, respectively (assuming that half of the stars are in front of the dust layer, and half behind it). Note that on average, the reddening values of Schlegel et al. agree very well with our estimates for GCs given in Gratton et al. (1997), with only a small scatter of ± 0.018 mag.

Foreground and internal reddenings have also been estimated from UBV photometry of individual early type stars by Oestreicher, Gochermann & Schmidt-Kaler (1995) and Oestreicher & Schmidt-Kaler (1996). The values for the directions of the two fields are: foreground: $E(B-V)=0.056$ and 0.062 ; internal: 0.150 and 0.140 . Again assuming that half of the stars are in front of the dust layer and half behind it, the average reddenings given by these maps are $E(B-V)=0.131$ and 0.132 for field A and B, respectively.

Much smaller reddenings are obtained by considering individual Cepheids. Reddenings for individual Cepheids have been given by Caldwell & Coulson (1986) and Gieren, Fouqué & Gomez (1998); these are the values used by Laney & Stobie (1994) and most works on Cepheids. The two sets of reddenings are on the same system (they are coincident for most of the stars in common). A weighted average of these reddening estimates (with weights proportional to the inverse square of the projected distance from our fields) yields mean reddening values of $E(B-V)=0.070$ for field A and 0.063 for field B. Note also that a star-by-star comparison shows that the reddening for the Cepheids are on average ~ 0.06 mag smaller than those given by the maps of Schlegel et al. (consistently with the result obtained for our fields).

Which of these two scales should be adopted?

Zaritsky (1999) noted that reddenings derived from early type stars may be biased towards large values, likely because these stars are preferentially located near star forming regions. However, quite clear indications for the reddening value to be adopted can be obtained directly from our RR Lyrae's. Before doing this, we note that a direct comparison of field A and B suggests that field A is slightly more reddened than field B. There are various consistent indications for this based on our data for the RR Lyrae's in the two fields:

- average colors of the *ab*, *c*, and *d*-type RR Lyrae's in field A are redder (by ~ 0.05 , 0.04 , and 0.03 mag respectively).
- on average, RR Lyrae's in field A are fainter by ~ 0.04 mag in V, and ~ 0.09 mag in B, compared to the variables in field B.

We conclude that reddening is likely to be 0.02 ± 0.01 mag larger in field A than in field B. This is quite consistent with the literature results mentioned above, and will be used in the following discussion when combining results from the two fields.

In our fields, reddening may be derived by comparing the edges of the instability strip defined by the RR Lyrae variables with e.g. that of M3 (as mentioned in Section 4.2 the RR Lyrae’s in the LMC have period and amplitude distributions more similar to those of the M3 variables, so that we can directly compare the average colors of the LMC RR Lyrae’s with those of the M3 ones). This same procedure was used by Walker (1992a) to constrain the reddening value in the LMC globular clusters he studied, thus allowing a more meaningful comparison between cluster and field variables.

Observed blue edges (in intensity averaged magnitudes) are 0.20 for M3 (Carretta et al. 1998), and about 0.24 mag for the LMC. Observed red edges are at 0.455 for M3, and 0.54 for the LMC (where we have corrected downward the colors of field A by 0.02 mag in order to be on the same system of field B). Averaging the differences between these two couple of values, we find that the reddening of the LMC should be 0.063 ± 0.023 larger than that for M3; this is about $E(B-V)=0.00$ (Ferraro et al. 1997). The reddening estimated from the RR Lyrae is then $E(B - V) = 0.063 \pm 0.023$ for field B, and $E(B - V) = 0.083 \pm 0.023$ for field A. These two values agree very well with the estimates based on Cepheids, but are much smaller than estimated from the Schlegel et al. reddening maps mentioned above (although they agree well with the estimates of the foreground reddening alone given by the two maps!)

Hereinafter, we will adopt reddening values of $E(B - V) = 0.06 \pm 0.02$ for field B, and $E(B - V) = 0.08 \pm 0.02$ for field A. Note that in this way reddenings for RR Lyrae are estimated consistently with those for Cepheids, so that we eliminated a possible source of inconsistency between distance scales. Furthermore, since we are using a large sample of ~ 100 objects projected into the direction of the bar, we also eliminated the possibility of systematic differences in the position of the barycentre, that is well possible when considering a small number of objects (like e.g. the globular clusters).

The absorption corrected intensity average magnitudes of the total sample of RR Lyrae’s with full coverage of the light curves are then $\langle V \rangle_0 = 19.116 \pm 0.017 \pm 0.062$ (average on 93 objects) and $\langle B \rangle_0 = 19.422 \pm 0.020 \pm 0.082$ (average on 81 objects) (where average values of each field are corrected for the corresponding reddening and adopting standard values for the selective absorption $A_V=3.1$ mag, $A_B=4.1$ mag according to Cardelli et al. 1989). Here the first error bar is the internal dispersion of the average, while the second term is due to the 0.02 uncertainty in the reddening, still by far the largest source of uncertainty. The final error should also include the contributions of the uncertainty of the photometric calibration and of the aperture corrections; they are basically given by the uncertainties of the calibrated magnitudes of the comparison stars (star #1253 in field A and star #128 in field B, see Table 2). Adding up in quadrature all error contributions we then get $\langle V \rangle_0 = 19.12 \pm 0.07$ (average on 93 objects) and $\langle B \rangle_0 = 19.42 \pm 0.10$ (average on 81

objects) for the average dereddened apparent luminosities of our sample of RR Lyrae’s in the bar of the LMC.

7. The clump

The clump method gives the shortest distance modulus to the LMC. Udalski et al. (1998) modulus of 18.08 ± 0.15 mag has undergone a number of revisions which have moved it towards longer values (18.18 ± 0.06 : Udalski 1998b; 18.23 ± 0.05 : Udalski 2000), but even the Popowski (2000) latest increase to 18.27 ± 0.06 still remains the shortest modulus derived so far for the LMC. It agrees with the short modulus provided by the eclipsing binaries method applied to two binaries in the LMC, HV2274 (Guinan et al. 1998b) and HV982 (Fitzpatrick et al. 2000). However, a more recent determination by Nelson et al. (2000) now gives a higher value of 18.40 ± 0.07 consistent with the original value of Guinan et al. (1998a: 18.42 ± 0.07), based on a more appropriate reddening determination for HV2274.

A lively discussion is taking place among scientists arguing whether the clump method is reliable or not, and invoking or not metallicity and age effects and dependences at various different extent. The clump method is based on I magnitudes. Although we did not observe in I, some hints on the clump issue can be drawn from the present photometry as well.

Hipparcos measured parallaxes for clump stars in the solar neighborhood and derived for them an absolute V magnitude of +0.8 mag (Jimenez, Flynn & Kotoneva 1998). This is 0.1 mag **fainter** than the absolute V magnitude of RR Lyraes at $[\text{Fe}/\text{H}] = -1.5$, the typical value for the LMC variables, if the absolute magnitude given by the statistical parallaxes and the B-W method is adopted.

We may check how well the mean absolute V magnitudes of the RR Lyrae and clump stars in the LMC bar compare by simply comparing their mean apparent magnitudes. This comparison is shown in Figure 14. In each panel of the figure boxes outline the clump stars of the field, chosen to lie in the region $B - V = 0.65 - 1.25$, and $V = 19.6 - 18.8$, and containing 5345 and 3639 stars in field A and B, respectively. The average magnitudes and colors of the clump stars are: $\langle B \rangle = 20.139$ mag, $\sigma = 0.219$, $\langle V \rangle = 19.223$ mag, $\sigma = 0.187$ mag, $\langle B \rangle - \langle V \rangle = 0.916$ mag in field A; and $\langle B \rangle = 20.126$ mag, $\sigma = 0.210$, $\langle V \rangle = 19.200$ mag, $\sigma = 0.185$ mag, $\langle B \rangle - \langle V \rangle = 0.926$ mag field B. The comparison with A97 average luminosity of the LMC clump (see their fig. 3) shows that our $\langle V_{\text{Clump}} \rangle$ is about 0.10 mag fainter.

The average apparent luminosity of the clump stars in the two fields is ~ 0.12 mag **brighter** than the RR Lyrae level (at a mean metallicity of $[\text{Fe}/\text{H}] = -1.5$). It is clear that the properties of the clump population are quite different in the LMC and in the solar neighborhood. This is not unexpected. However the differences in M_V are not those expected based on the OGLE results. To show this, we may transform our mean $\langle V \rangle$ magnitudes for the clump stars to mean $\langle I \rangle$ magnitudes. Udalski (1998b) lists $(V - I)_0$ colors for a number of clusters in the LMC obtained in

the second phase of the OGLE microlensing survey (OGLE-II, Udalski et al. 1997). This average value is $(V - I)_0 = 0.89 \pm 0.01$. If we now subtract this value from our $\langle V \rangle$'s, and apply a reddening correction of $E(V - I) = 0.11 \pm 0.02$ which is appropriate for our fields (obtained transforming our $E(B - V)$ values to $E(V - I)$ according to Cardelli et al. 1989 formulas), we obtain $\langle I \rangle = 18.21 \pm 0.03$, and $I_0 = 18.10 \pm 0.06$ with an absorption correction of $A_I = 0.11$.

Using the metallicity-I luminosity calibration for the clump stars by Udalski (2000; $M_I = 0.13([\text{Fe}/\text{H}] + 0.25) - 0.26$), and assuming a mean metallicity of $[\text{Fe}/\text{H}] = -0.55$ (again as in Udalski 2000), we find a distance modulus of $(m - M)_{0,\text{LMC}} = 18.40 \pm 0.07$; while if we adopt instead the calibration by Popowski (2000) we obtain $(m - M)_{0,\text{LMC}} = 18.44 \pm 0.07$. These values are larger than those found by Udalski (2000) and Popowski (2000), although in agreement with almost all other distance modulus determinations for the LMC (see Figure 1). Note that given the low sensitivity of M_I on metallicity, the assumption about the metal abundance of the clump stars has little impact on this distance derivation.

Why our result is different from those obtained by Udalski and Popowski? the adopted average $V - I$ for the clump stars is not likely to be the reason. In fact, in order to find an $\langle I \rangle$ magnitude as bright as that required to produce a distance modulus as short as that obtained by these authors, we would have to adopt a redder $(V - I)_0$ color of ~ 1.0 mag for the clump of the LMC, similar to that found for the clump stars in the solar neighborhood. This is inconsistent with the lower metallicity of the LMC (and the same Udalski's results). The difference seems rather due to the bright I and V magnitudes found by OGLE. Note also that if the distance modulus of the LMC by Udalski (2000) were correct, then according to our V average apparent luminosity and reddening values for the RR Lyrae's in the LMC, the average absolute magnitude of the RR Lyrae's at $[\text{Fe}/\text{H}] = -1.5$ would be as faint as $M_V = 0.89$, much lower than found for the absolute magnitude of the Horizontal Branch stars from Hipparcos parallaxes (Gratton 1998), and than the values given by the statistical parallaxes and the B-W method (already fainter than those derived by other techniques). We would have to claim the existence of systematic differences between RR Lyrae in our Galaxy and in the LMC!

Since we do not have independent I photometry we are not able to check whether Udalski (1998b) $(V - I)_0 = 0.89 \pm 0.01$ is correct or not. Our feeling is that both OGLE-II V and I magnitudes may be too bright compared with the Johnson values (perhaps due to differences between OGLE-II and Johnson photometric systems), but if OGLE-II V and I are both overestimated of approximately the same amount, then the $(V - I)_0 = 0.89$ mag we have used may be correct, and so also our above conclusions about the distance modulus of the LMC derived from the clump method.

In any case, although we are not able to completely settle this issue, we think that this exercise supports our conclusion that the distance modulus of the LMC derived from the clump stars is still rather uncertain.

8. Comparison with previous photometric results

The average absorption corrected apparent V luminosity of the 93 single-mode RR Lyrae’s with full coverage of the light curve in our sample is $\langle V(\text{RR}) \rangle_0 = 19.12 \pm 0.02 \pm 0.03 \pm 0.06$ at an average metallicity of $[\text{Fe}/\text{H}] = -1.5$ (Bragaglia et al. 2000) and for an average reddening value of 0.07 mag (see Section 6). Here 0.02 mag is the standard deviation of the average, 0.03 mag is the photometric zero point contribution, and 0.06 mag is the absorption contribution due to the 0.02 mag uncertainty in the reddening.

This value is to be compared with the following estimates available in the literature: (i) $\langle V(\text{RR}) \rangle_0 = 18.94 \pm 0.04$, Walker (1992a), based on 182 variables in 7 LMC globular clusters at $[\text{Fe}/\text{H}] = -1.9$ and for an average reddening value of $\langle E(B-V) \rangle = 0.9$ mag. The 0.04 mag error bar is the internal error and Walker (1992a) estimates that systematic errors due to photometric zero points and absorption are of the order of 0.02–0.03 and 0.05 mag, respectively; (ii) $\langle V(\text{RR}) \rangle_0 = 19.09$, A96, from a sample of 500 RR Lyrae’s observed by the MACHO microlensing experiment, at $[\text{Fe}/\text{H}] = -1.7$ and for $E(B-V) = 0.10$ mag, according to Bessell (1981). A96 quote ± 0.07 mag as the mean error of a single point on the light curve, while A97 attach an error of 0.10 mag as a conservative estimate of the MACHO photometric uncertainties⁶; and (iii) $\langle V(\text{RR}) \rangle_0 = 18.94 \pm 0.04$ mag at $[\text{Fe}/\text{H}] = -1.6$ and for an assumed reddening value of 0.12 mag, Udalski et al. (1999).

Since the luminosity of the RR Lyrae variables depends on metallicity, the above values must be referred to a common value of $[\text{Fe}/\text{H}]$ in order to compare them. We have transformed all literature values to a common metallicity value of $[\text{Fe}/\text{H}] = -1.5$ (this is also the most commonly adopted average value for the LMC), using a slope of 0.2 mag/dex for the luminosity metallicity relation of the RR Lyrae variables (see Introduction). In Table 4 we summarize the $\langle V(\text{RR}) \rangle_0$ values from the literature transformed to $[\text{Fe}/\text{H}] = -1.5$, and we also list the associated errors divided in internal contribution and systematic errors (photometric zero point and absorption components).

A96 do not provide a specific evaluation of all error contributions and we have worked them out as follows: (i) we estimate a 0.073 mag photometric zero point uncertainty based on the combination of A99 0.021 mag internal precision of the MACHO photometry, and $A96 \pm 0.07$ mag mean error of a single point of the RR Lyrae photometry; and (ii) the 0.06 absorption uncertainty is again our guess based on a 0.02 uncertainty in the reddening. Finally, the 0.10 mag total error is likely to be an underestimate since it does not include the standard deviation of the average (not provided by A96), however accidentally coincides with A97 conservative estimate of the photometric uncertainties of MACHO photometry for the RR Lyrae’s.

⁶More recently A99 published a detailed description of the photometric calibration of the twenty top-priority MACHO fields of the LMC (which include fields #6 and #13). They quote an internal precision of the MACHO photometry calibration of $\sigma_V = 0.021$ mag (based on 20,000 stars with $V \lesssim 18$ mag) and, from the comparison with other published measurements, they estimate a mean offset between MACHO and all of the other data of $\delta V = -0.035$ mag (see fig. 7 of that paper).

Within the quoted uncertainties the present photometry agrees well with Walker (1992a), particularly if NCG 1841, the cluster suspected to be about 0.2 mag closer to us (Walker 1992a) is discarded, thus ruling out the existence of any intrinsic differences between field and cluster variables. Walker’s and our photometries are both on the same consistent Johnson photometric system, and based on reddenings values measured with the very same procedure based on the intrinsic properties of the stars which average luminosities are compared. Noteworthy Walker’s (1992a) and our reddening values coincide, and are in perfect agreement with the Cepheids estimated reddening when NGC 1841 is discarded.

The comparison with MACHO and OGLE-II photometries is made more complicated by the differences in the adopted reddening values (with MACHO and OGLE-II reddenings being 0.03 and 0.05 mag larger than our average value, respectively) which may well hide or mimic differences between photometric systems.

A direct comparison between MACHO’s and our photometry on a star by star basis is in principle possible, since we observed RR Lyrae’s in the same areas and thus with same reddening. For the time being this is only feasible for the 9 RRd’s in common with A97 for which calibrated $\langle V \rangle$ are published in tab. 1 of A97. We find that the average difference in V (this paper — A97) is $\Delta V = 0.15 \pm 0.04$ ($\sigma = 0.13$ - 9 stars) and may reduce to 0.12 if A97 are magnitude average instead of intensity average values.

This value should provide an estimate of the systematic differences existing between MACHO and our photometry (with MACHO photometry being systematically *brighter* by about 0.1 mag) possibly due to the nonstandard filters of MACHO. We remind however that our data sampling of the RRd’s light curves is much poorer than in MACHO.

On the other hand, if we adopt the $\langle V \rangle = 19.4$ mag value of the mean apparent magnitude of the total sample of 500 RR Lyrae’s in A96 and compare it with our mean apparent magnitude of 19.33 (average on 93 single-mode RR Lyrae’s) we would conclude instead that MACHO magnitudes are systematically fainter by about 0.07 mag than our values!

A truly meaningful comparison will be possible only when final calibrated light curves for the MACHO RR Lyrae’s in field #6 and #13 will be made available to the astronomical community.

Udalski et al. (1999) OGLE-II dereddened average luminosity of the RR Lyrae stars in the bar of the LMC is systematically brighter by 0.16, 0.13 and 0.10 mag (or 0.06 mag if NGC1841 is included) than the present photometry, A96 and Walker (1992a), respectively. The total error bar of Udalski et al. (1999) data only marginally allows to make their $\langle V(RR) \rangle_0$ overlap with the estimate from the present photometry. In order to make the two estimates coincide, the reddening of Udalski et al. (1999) should be lowered to 0.07 mag, a too small value perhaps, since Udalski et al. LMC fields containing the RR Lyraes are centered on the LMC bar. Our results for the RR Lyrae’s and the clump stars seem to suggest instead that the too bright OGLE-II V (and I) magnitudes

could partially be due to differences between Johnson and OGLE-II photometric systems. OGLE-II data for the LMC come from driftscan mode observations with effective exposure times of 180^s and 240^s at V and B, respectively. Udalski et al. (1998) compared their LMC photometry of Cepheid variables in NGC 1850, with that of Sebo and Wood (1995), apparently the only reliable CCD photometry existing of regions overlapping with OGLE-II LMC fields. They only show the comparison in the I band (see their fig. 1) and conclude that the zero points of the OGLE-II magnitude scale (0.01 and 0.015 mag for the I and V bands, respectively) are correct. However, Cepheids in their fig. 1 are about 5-7 mag brighter than the luminosity level of the RR Lyrae and clump stars in the bar of the LMC. Thus from this comparison the existence of any systematic differences at the faint magnitude level of the LMC RR Lyrae and clump stars cannot be ruled out.

9. Summary and conclusions

We have presented new B and V photometry in the Johnson system obtained for two fields close to the bar of the LMC and partially overlapping with fields #6 and #13 of the MACHO microlensing experiment. 128 RR Lyrae variables, 11 Cepheids, 12 eclipsing binaries and 1 δ Scuti star have been identified in the two areas. The new photometry allows a very precise estimate of the average V and B apparent luminosity of the RR Lyrae variables, as well as of the clump stars. An estimate of the reddening within the two fields was also obtained from the colors of the edges of the instability strip defined by the RR Lyrae variables. This corresponds to $E(B-V)=0.08$ and 0.06 mag in field A and B, respectively. The average dereddened apparent luminosity of the RR Lyrae and clump stars is $\langle V(RR) \rangle_0 = 19.12 \pm 0.07$ and $\langle V_{\text{clump}} \rangle_0 = 18.99 \pm 0.07$, where errors include standard deviation, photometric zero point and absorption contributions.

The present $\langle V(RR) \rangle_0$ moves the B-W and statistical parallaxes determinations of the distance modulus of the LMC to 18.44 ± 0.15^7 and 18.36 ± 0.12 , respectively.

The present determination of the V luminosity of the clump stars when combined with OGLE-II $\langle V - I \rangle_0 = 0.89$ mag and corrected back to our new reddening values leads to $\langle I \rangle_0 = 18.10 \pm 0.07$ mag and moves the clump distance modulus of the LMC to 18.40 ± 0.07 and 18.44 ± 0.07 mag, when Udalski (2000) or Popowski (2000) metallicity-I luminosity relations for the clump stars are adopted.

Carretta et al. (2000b) provide a synthesis of the distance moduli to the LMC given by different distance indicators, which is the main source of the data shown in panels (a) and (b) of Figure 1. The distance moduli for the LMC from B-W, statistical parallaxes and clump methods based on the present new photometry and reddening are shown as stars in panel (b) of Figure 1.

⁷The B-W value would further move to 18.56 mag using the new preliminary estimate of the magnitude of the Galactic field RR Lyrae variable RR Cet: $M_V(RR) = 0.56$ mag at $[Fe/H] = -1.5$, from Cacciari et al. (2000) revision of the B-W method.

Further changes with respect panel (a) are (i) Nelson et al. (2000) revised estimate of the distance to the LMC from the eclipsing binary system HV 2274, based on new reddening determinations for this star, which has moved the distance back to the original value by Guinan et al. (1998a) giving $\mu_{\text{LMC}}=18.40\pm0.07$, and (ii) Panagia (1998) latest marginal revision of the SN1987A estimate: $\mu_{\text{LMC}}=18.55\pm0.05$

”All” distance determinations converge within 1σ on a distance modulus of $\mu_{\text{LMC}}=18.50\pm0.03\pm0.06$ mag (where the first error bar is the 1σ scatter of the average, and the second error is the absorption contribution due to the 0.02 mag uncertainty in the reddening), thus allowing to fully reconcile the *long* and a *short* distance scale to the LMC. This value is shown by the solid line of Figure 1b, while dashed lines give the $1\sigma=0.07$ mag errorbars.

Note that this result mainly stems from the use of a consistent reddening scale for RR Lyrae and Cepheids in the LMC.

An implicit conclusion of this discussion is that the correct magnitude scale for GCs RR Lyrae’s is midway between those given by statistical parallaxes and MS fitting; this implies ages of 13-14 Gyr for the GCs.

We warmly thank P. Montegriffo for his expert advice during the reduction phase, for the use of his software, and for the development of the specific software used for the detection of the variable stars and in the study of their periodicities. A special thanks goes to M.Marconi who performed helpful theoretical checks of the classification, according to Bailey types, of some of the RR Lyrae variables. We are indebted to G. Rodighiero for her advice on the use of SExtractor, to M. Bellazzini and M. Messineo for their advice in setting the DoPHOT reductions, and to R. Merighi for help in the layout of some of the figures of the paper. This work was partially supported by MURST - Cofin98 under the project ”Stellar Evolution.”

REFERENCES

- Alcock, C. *et al.* (the MACHO collaboration) 1996, AJ, 111, 1146 (A96)
 Alcock, C. *et al.* (the MACHO collaboration) 1997, ApJ, 482, 89 (A97)
 Alcock, C. *et al.* (the MACHO collaboration) 1999, PASP, 111, 1539 (A99)
 Barning, F.J.M. 1962, Bull. Astron. Inst. Netherlands, 17, 22
 Bertin, E., Arnouts, S. 1996, A&AS, 117, 393
 Bessel, M.S. 1991, A&A, 262, L17
 Bingham, E.A., Cacciari, C., Dickens, R.J., & Fusi Pecci, F. 1984, MNRAS, 209, 765
 Bono, G., Caputo, F., Castellani, V., & Marconi, M. 1997, A&AS, 121, 327
 Bono, G., Caputo, F., Cassisi, S., Incerpi, R., & Marconi, M. 1997, ApJ, 483, 811

- Bragaglia, A., Gratton, R.G., Carretta, E. Clementini, G., Di Fabrizio, & Marconi, M. 2000, AJ, submitted
- Cacciari, C., Clementini, G., Castelli, F., & Melandri, F. 2000, in *The Impact of Large Scale Surveys on Pulsating Stars Research*, Eds. L. Szabados & D. Kurtz, APS Conf. Ser. Vol 203, 176
- Cacciari, C., Clementini, G., Castelli, F. 2000, in preparation
- Caldwell, J.A.R., & Coulson, I.M. 1986, MNRAS, 218, 233
- Caloi, V., D’Antona, F., & Mazzitelli, I. 1997, A&A, 320, 823
- Canuto, V., & Mazzitelli, I. 1992, ApJ, 389, 724
- Cardelli, J.A., Clayton, G.C., & Mathis, J.S. 1989, ApJ, 345, 245
- Carney, B.W., Storm. J., & Jones, R.W. ApJ, 386, 663
- Carretta, E., Gratton, R.G., & Clementini G. 2000a, MNRAS, in press (astro-ph/0001526)
- Carretta, E., Gratton, R.G., Clementini G., & Fusi Pecci, F. 2000b, ApJ, 533, 215
- Carretta, E., Cacciari, C., Ferraro, F.R., Fusi Pecci, F., & Tessicini, G. 1998, MNRAS, 298, 1005
- Catelan, M. 1998, ApJ, 495, L81
- Castelli, F. 1999, A&A, 346, 564
- Chaboyer, B., Demarque, P., Kernan, P.J., & Krauss, L.M. 1998, ApJ, 494, 96
- Corsi, C.E., Rich, M., Cacciari, C., Federici, L., & Fusi Pecci, F. 2000, in *A Decade of HST Science*, Ed. M. Livio, STScI Publications, in press
- Di Benedetto G.P. 1997, ApJ, 486, 60
- Di Fabrizio, L. Clementini, G., Gratton, R.G., Carretta, E., & Bragaglia, A. 2000, A&A, submitted
- Djorgovski, S.G. 1993, ASP Conf. Ser. 50, 373
- Feast, M.W., & Catchpole, R.M. 1997, MNRAS., 286, L1
- Fernley, J. 1994, A&A, 284, L16
- Fernley, J., Barnes, T.G., Skillen, I., Hawley, C.J., Hanley, C.J., Evans, D.W., Solano, E., & Garrido, R. 1998a, A&A, 330, 515
- Fernley, J., Carney, B.W., Skillen, I., Cacciari, C., & Janes, K. 1998b, MNRAS, 293, L61
- Ferraro, R.R., Carretta, E., Corsi, C.E., Fusi Pecci, F., Cacciari, C., Buonanno, R., Paltrinieri, B., & Hamilton, D. 1997, A&A, 320, 757
- Fitzpatrick, E.L., Ribas, I., Guinan, E.F., DeWarf, L.E., Maloney, F.P., & Massa, D.L. 2000, AAS 196, 2806
- Fusi Pecci, F. et al. 1996, AJ, 112, 1461
- Gieren, W.P., Fouqué, P., & Gómez, M. 1998, ApJ, 496, 17
- Gould, A., & Popowski, P. 1998, ApJ, 508, 844

- Gratton, R.G. 1998, MNRAS, 296, 739
- Gratton, R.G., Sneden, C., Carretta, E., & Bragaglia, A. 2000, A&A, 354, 169
- Gratton, R.G., Fusi Pecci, F., Carretta, E., Clementini, G., Corsi, C.E., & Lattanzi, M. 1997, ApJ, 491, 749
- Guinan, E.F., Ribas, I., Fitzpatrick, E.L., & Pritchard, J.D. 1998a, in *Ultraviolet Astrophysics Beyond the IUE Final Archive*, ed. W. Wamsteker, R. Gonzalez-Riestra, & B. Harris (ESA SP-413) (Noordwijk:ESA), 315
- Guinan, E.F., Ribas, I., Pritchard, J.D., Bradstreet, D.H., & Gimenez, A. 1998b, ApJ, 509, L21
- Jimenez, R., Flynn, C., & Kotoneva, E. 1998, MNRAS, 299, 515
- Jones, R.V., Carney, B.W., Storm, J., & Latham, D.W. 1992, ApJ, 386, 646
- Kurucz, R.L. 1995, available at <http://cfaku5.harvard.edu>
- Kinman, T.D., Stryker, L.L., Hesser, J.E., Graham, J.A., Walker, A.R., Hazen, M.L., & Nemec, J.M. 1991, PASP, 103, 1279
- Landolt, A.U. 1992, AJ, 104, 340
- Laney, C.D., & Stobie, R.S. 1994, MNRAS, 266, 441
- Liu, T., & Janes, K.A. 1990, ApJ, 354, 273
- Lomb, N.R. 1976, Ap&SS, 39, 447
- Nelson, C.A., Cook, K.H., Popowski, P., & Alves, D.R. 2000, AJ, 119, 1205
- Oestreich, M.O., Gochermann, J., & Schmidt-Kaler, T. 1995, A&A, 112, 495
- Oestreich, M.O., & Schmidt-Kaler, T. 1996, A&AS, 117, 303
- Oosterhoff, P.Th. 1939, Observatory, 62, 104
- Panagia, N. 1998, in Proceedings of IAU Symposium 190, on *New views of the Magellanic Clouds*, p. 53
- Panagia, N., Gilmozzi, R., & Kirshner, R.P. 1998, in *SN 1987A: Ten Years After*, edited by M. Phillips & N. Suntzeff (San Francisco: ASP), in press
- Petersen, J.E. 1973, A&A, 27, 89
- Popowski, P. 2000, ApJ, 528, L9
- Preston, G.W. 1959, ApJ, 130, 507
- Sandage, A. 1990, ApJ, 350, 603
- Sandage, A. 1993, AJ, 106, 703
- Scargle, J.D. 1982, ApJ, 263, 835
- Schechter, P.L., Mateo, M., Saha, A. 1993, PASP, 105, 1342
- Schlegel, D.J., Finkbeiner, D.P., & Davis, M., 1998, ApJ, 500, 525

- Schommer, R.A., Olszewski, E.W., Suntzeff, N.B., & Harris, H.C 1992, *AJ*, 103, 447
- Sebo, K.M., & Wood, P.R. 1995, *ApJ*, 449, 164
- Skillen, I., Fernley, J., Stobie, R.S., & Jameson, R.F. 1993, *MNRAS*, 265, 301
- Sweigart, A. 1997, *ApJ*, 474, L23
- Tsujimoto, T., Miyamoto, M., & Yoshii, I. 1998, *ApJ*, 492, L79
- Udalski, A. 1998a, *Acta Astronomica*, 48, 113
- Udalski, A. 1998b, *Acta Astronomica*, 48, 383
- Udalski, A. 2000, *ApJ*, 531, L25
- Udalski, A., Kubiak, M., Szymański, M. 1997, *Acta Astronomica*, 47, 319
- Udalski, A., Szymański, M., Kubiak, M., Pietrzyński, G., Soszyński, I., Woźniak, P., & Zebruń, K. 1999, *Acta Astronomica*, 49, 201
- Udalski, A., Szymański, M., Kubiak, M., Pietrzyński, G., Woźniak, P., & Zebruń, K. 1998, *Acta Astronomica*, 48, 1
- Van Leeuwen, F., Feast, M.W., Whitelock, P.A., & Yudin, B. 1997, *MNRAS*, 287, 955
- Walker, A.R. 1992a, *ApJ*, 390, L81
- Walker, A.R. 1992b, *AJ*, 103, 1166
- Walker, A.R. 1992c, *AJ*, 104, 1395
- Zaritsky, D. 1999, *ApJ*, 118, 2824

Table 1: Number of variables identified in our fields

	Field A	Field B	Total
RRab	48	31	79
RRc	21	18	39
RRd	6	4	10
Cepheids	10	1	11
Binaries	7	5	12
δ Scuti	1	—	1
Total	93	59	152
Candidate variables	5	5	10

Table 2: Coordinates and magnitudes of the comparison stars

Number	α	δ	V	n_V	B	n_B
Field A						
1253	5 22 58.22	−70 31 32.07	16.80±0.03	18	17.48±0.04	10
1550	5 23 08.42	−70 28 50.59	16.76±0.03	18	18.43±0.04	10
879	5 22 50.71	−70 34 46.50	17.06±0.03	18	18.45±0.04	10
9101	5 22 53.17	−70 29 50.30	19.40±0.03	18	20.36±0.04	10
Field B						
128	5 16 29.80	−71 01 43.16	16.18±0.03	9	16.85±0.05	3
346	5 17 28.94	−71 04 34.74	16.96±0.03	9	18.39±0.05	3
531	5 17 25.04	−71 02 38.26	18.15±0.03	9	19.19±0.05	3
4340	5 18 08.17	−71 00 41.17	19.30±0.03	9	20.22±0.05	3

Table 3: Intensity average magnitudes of the double-mode variables in our sample

Identifier (this paper)	Identifier (Di Fabrizio et al. 2000)	Identifier (A97)	P ₁ (A97)	<V>	<V> (A97)	
2249	201	—	0.3063*	19.32	—	19.68
23032	202	CA02-13.6691.4052	0.34226	19.67	19.28	20.14
7137	203	CA05-13.7054.2970	0.34301	19.38	19.15	19.76
8654	204	CA12-06.6933.939	0.34544	19.15	19.16	19.51
7467	205	CB45-13.6080.591	0.35775	19.01	18.94	19.32
4420	206	CA48-06.6811.651	0.35989	19.35	19.25	19.71
3347	207	CB49-13.5836.525	0.36040	19.19	19.02	19.52
6470	208	CB59-13.5838.497	0.36979	19.18	19.08	19.53
4509	209	CB61-13.5958.518	0.37130	19.49	19.21	19.88
3155	210	CA67-06.6810.428	0.38141	19.14	19.08	19.54

*P₁ for #2249 is from the present photometry

Table 4: Comparison with the $\langle V(RR) \rangle_0$ values in the literature transformed to a common value of the metallicity: $[Fe/H]=-1.5$

$\langle V(RR) \rangle_0$	N_{stars}	Error				Reddening	Reference
		(1)	(2)	(3)	(total)		
19.12	93	0.02	0.03	0.06	0.07	0.07	This paper
19.02	182	0.04	0.025	0.05	0.07	0.09	Walker (1992a)
19.06 ^a	160	0.04	0.025	0.05	0.07	0.07	Walker (1992a)
19.095 ^b	500	–	0.073 ^c	0.06 ^c	0.10 ^c	0.10	A96–MACHO
18.96	104	0.04	0.015 ^d	0.08 ^d	0.09	0.12	Udalski et al. (1999)–OGLE II

(1)= standard deviation of the average, (2)=photometric zero point, (3)= absorption contribution

^aAverage value without NGC1841

^bFrom A96 19.09 value corrected for both the metallicity effect (+0.04 mag) and the $\delta V=-0.035$ mag shift existing between MACHO and the literature data (see A99)

^cThese errors are our guess, according to the procedure described in Section 8

^dSources for the photometric zero point and absorption contributions to the total error are Udalski et al. (1998) and Udalski (1998a), respectively

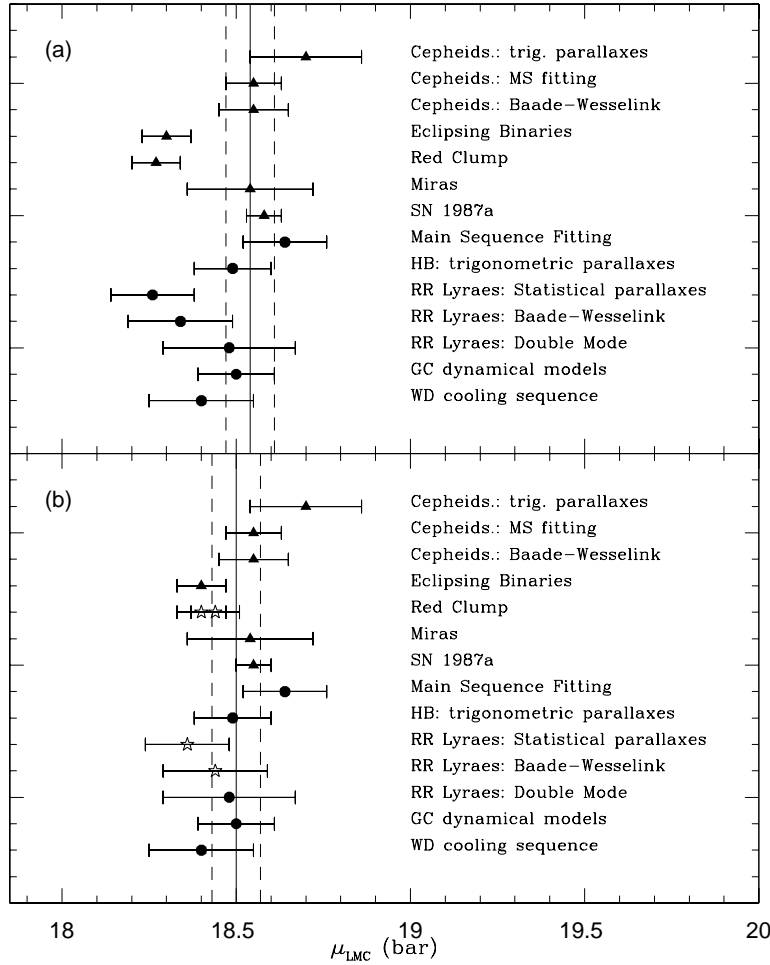


Fig. 1.— The distance modulus of the Large Magellanic Cloud as derived from various distance indicators. Triangles and circles mark the Population I and II indicators, respectively. Data in panel (a) of the figure for the Cepheids are taken from: (a) trigonometric parallaxes, Feast & Catchpole (1997; with errorbar revised according to Carretta et al. 2000b); (b) MS Fitting, Laney & Stobie (1994; with errorbar revised according to Carretta et al. 2000b); (c) B-W, average of Gieren et al. (1998) and Di Benedetto (1997; see Carretta et al. 2000b); for the eclipsing binaries from: Guinan et al. (1998b) and Fitzpatrick et al. (2000); for the clump from: Popowski (2000); for the Miras from: Van Leeuwen et al. (1997); for SN1987a from: Panagia, Gilmozzi & Kirshner(1998); for the MSF and the HB stars from: Carretta et al. (2000b); for the RR Lyrae Statistical parallaxes and B-W: from $M_V(RR)=0.76$ and 0.68 mag, respectively and Walker (1992a) $\langle V(RR) \rangle_0$ and reddening values (see Introduction); for the LMC RRd's from: A97; for the GCs dynamical models from: Carretta et al. (2000b) revision of Chaboyer et al. (1998); and for the white dwarfs cooling sequence from: Carretta et al. (2000b). The solid and dashed lines in panel (a) represent Carretta et al. (2000b) preferred value $\mu_{LMC}=18.54$ and its $1\sigma=0.07$ mag errorbar. The distance moduli for the LMC from B-W, statistical parallaxes and clump methods based on the present new photometry and reddening are shown as stars in panel (b) of Figure 1. Further changes with respect to panel (a) are (i) Nelson et al. (2000) revised estimate of the distance to the LMC from the eclipsing binary system HV 2274: $\mu_{LMC}=18.40\pm0.07$, and (ii) Panagia (1998) latest estimate from SN1987A: $\mu_{LMC}=18.55\pm0.05$. The solid and dashed lines in panel (b) show our preferred value $\mu_{LMC}=18.50$ and its $1\sigma=0.07$ mag errorbar (see Section 9).

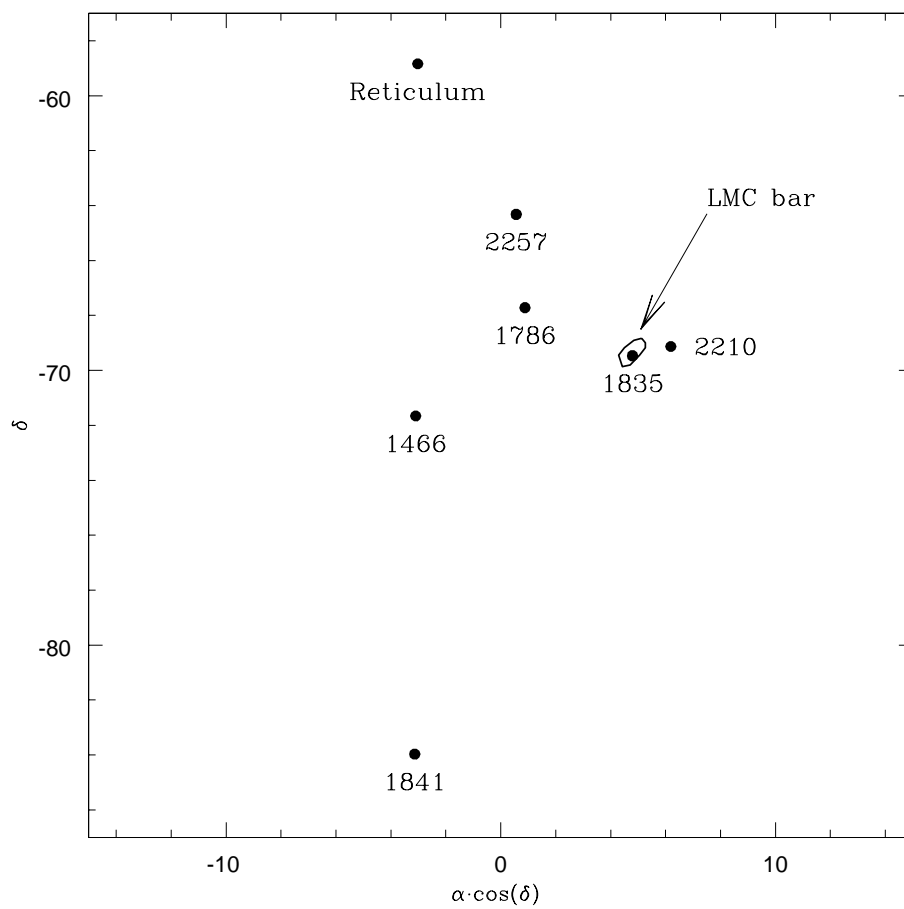


Fig. 2.— Positions of the 7 LMC globular clusters studied by Walker (1992a) with respect to the LMC bar.

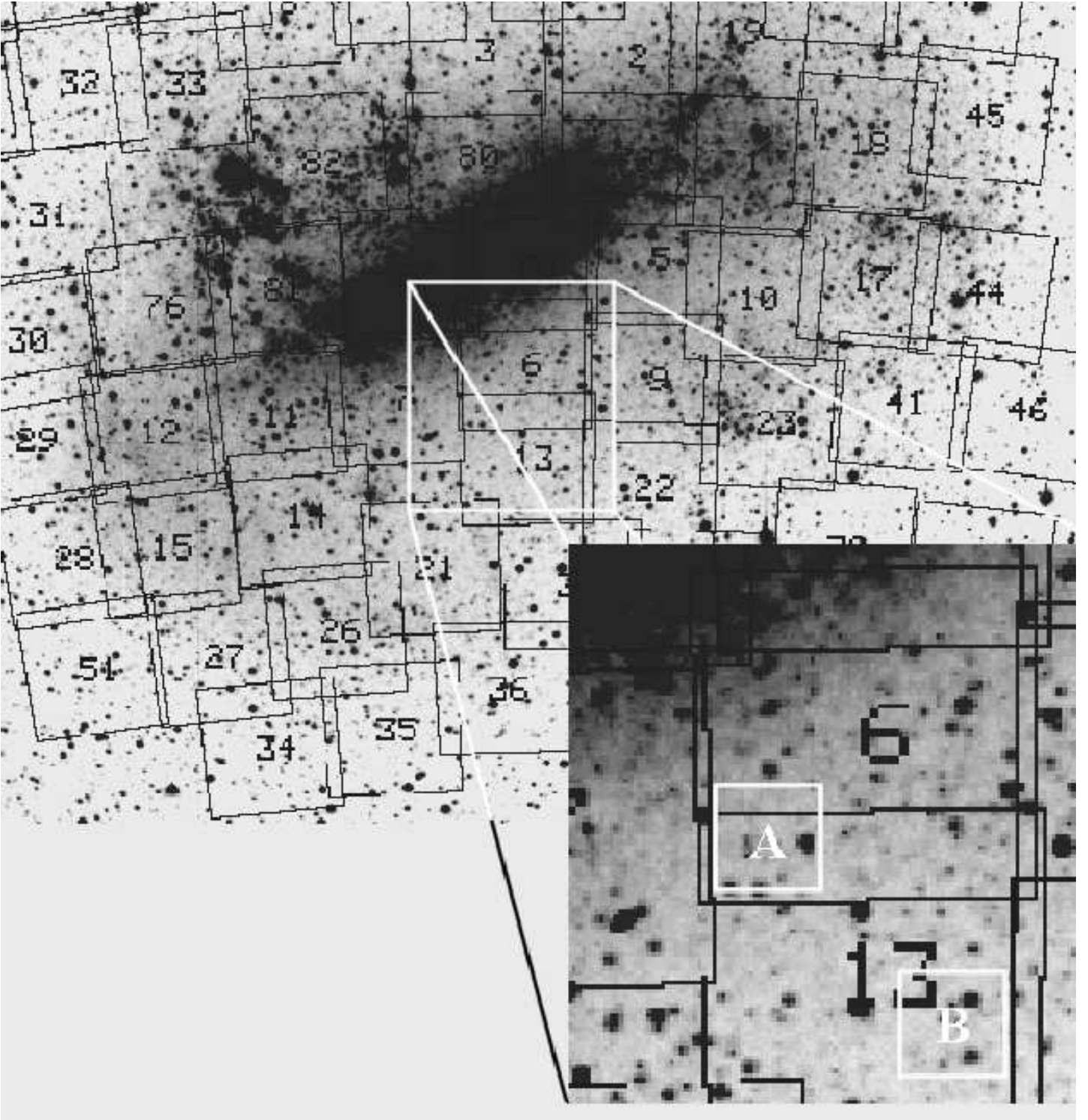


Fig. 3.— Observed fields and their positions with respect to MACHO’s fields.

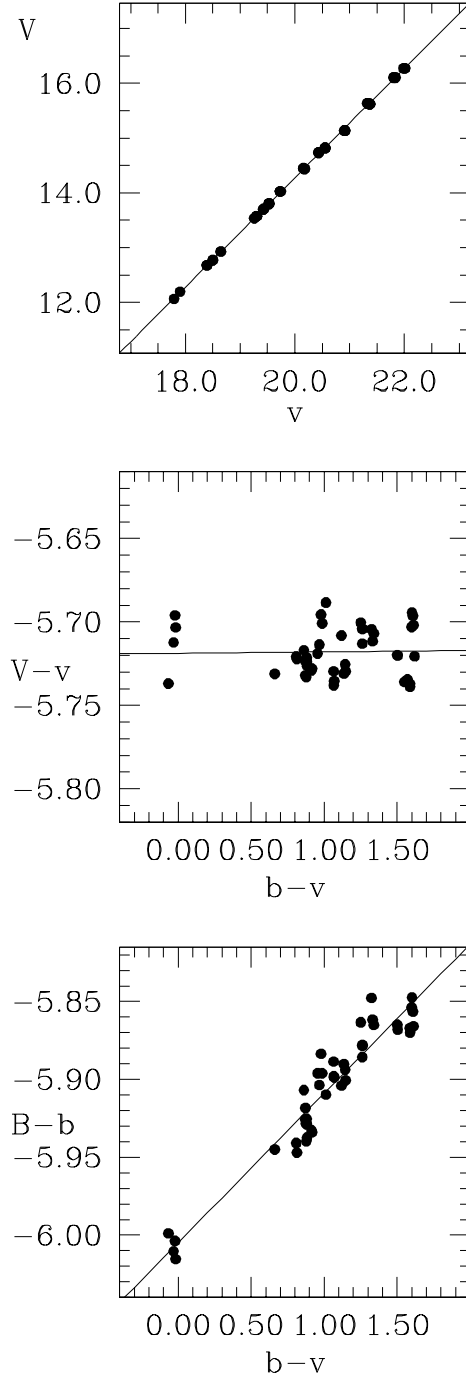


Fig. 4.— Calibration equations

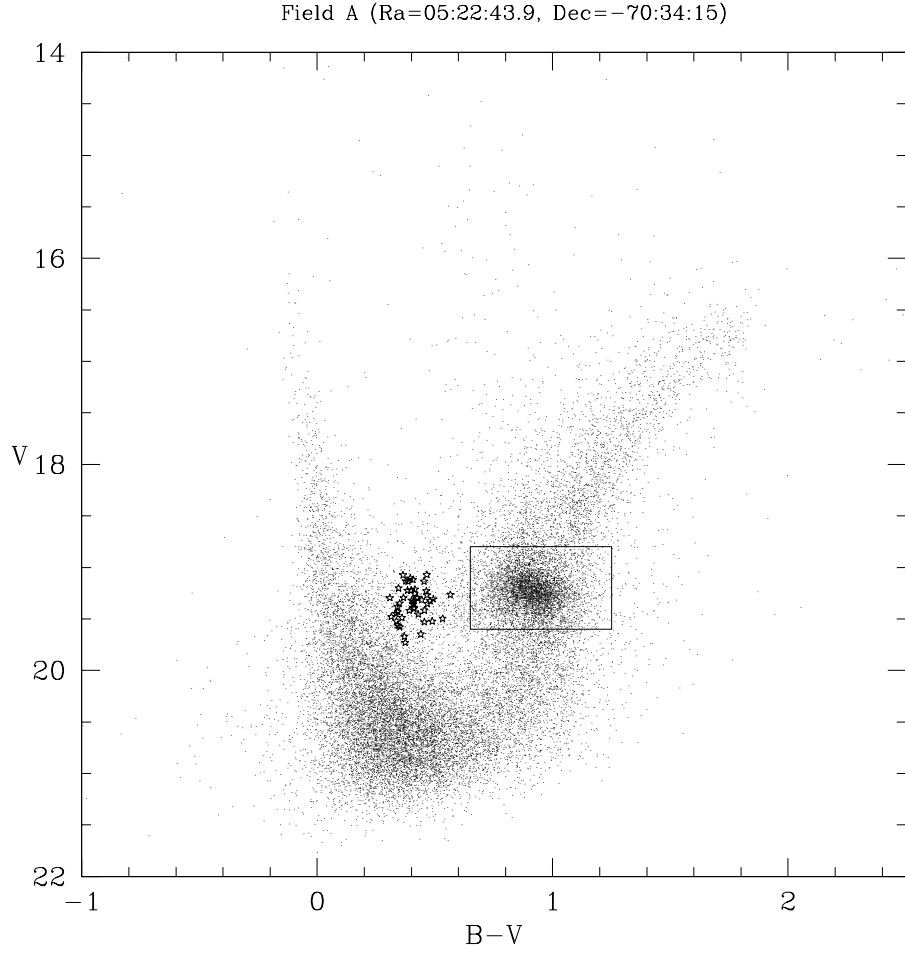


Fig. 5.— HR diagrams of field A. The box outlines the clump stars of this field, chosen to lie in the region with $B-V=0.65-1.25$, and $V=19.6-18.8$ and containing 5345 stars (see Section 7). Stars mark the RR Lyrae variables identified in this field which have full coverage of the V and B light curves (47 objects), plotted according to their intensity average magnitudes and colors ($\langle V \rangle$, $\langle B \rangle - \langle V \rangle$).

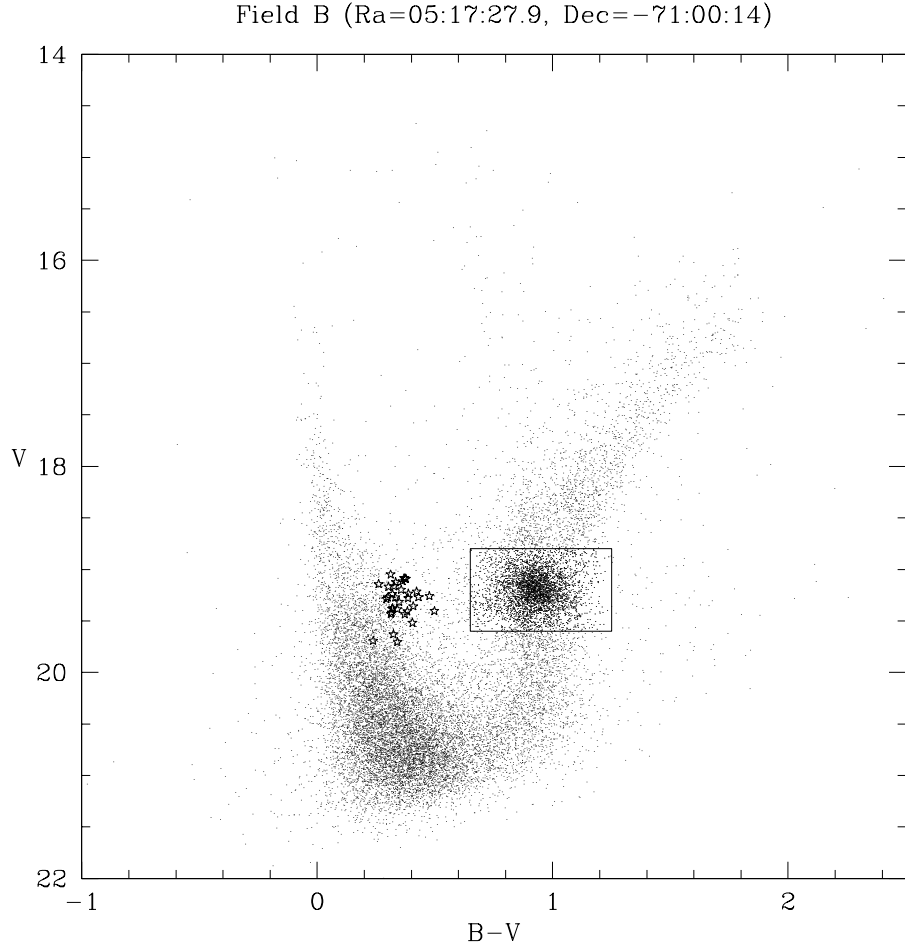


Fig. 6.— HR diagrams of field B. The box outlines the clump stars of the field, chosen to lie in the region with $B-V=0.65-1.25$, and $V=19.6-18.8$ and containing 3639 stars (see Section 7). Stars mark the RR Lyrae variables identified in this field which have full coverage of the V and B light curves (33 objects), plotted according to their intensity average magnitudes and colors ($\langle V \rangle$, $\langle B \rangle - \langle V \rangle$).

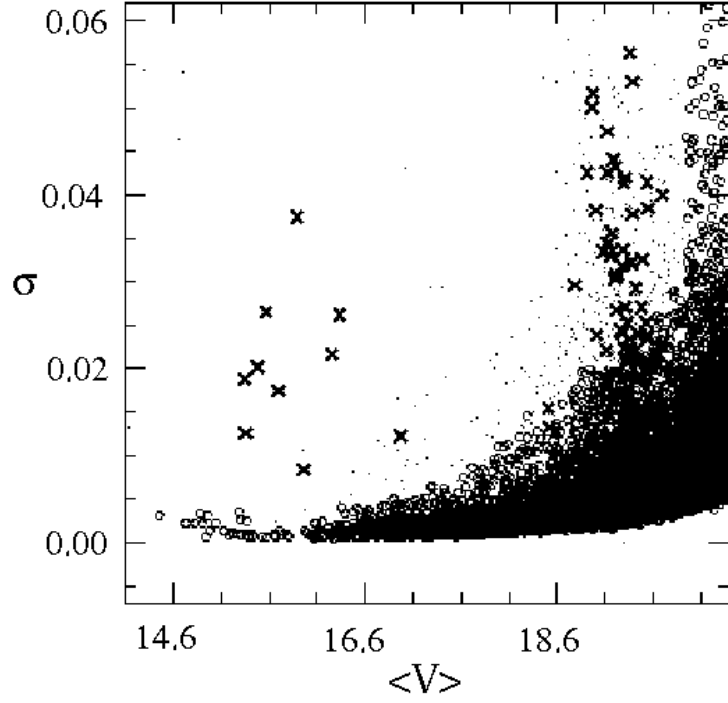


Fig. 7.— σ vs $\langle V \rangle$ -magnitude plot of the stars in field A produced by the program VARFIND. 28,638 objects are displayed in the full plot. Crosses mark the variables identified in this field (93 objects). The region at $18.6 < V < 19.8$ mag corresponds to the RR Lyrae variables, while variables around $15.1 < V < 16.6$ mag are Cepheids. Dots plot all the objects checked for variability in field A (1165).

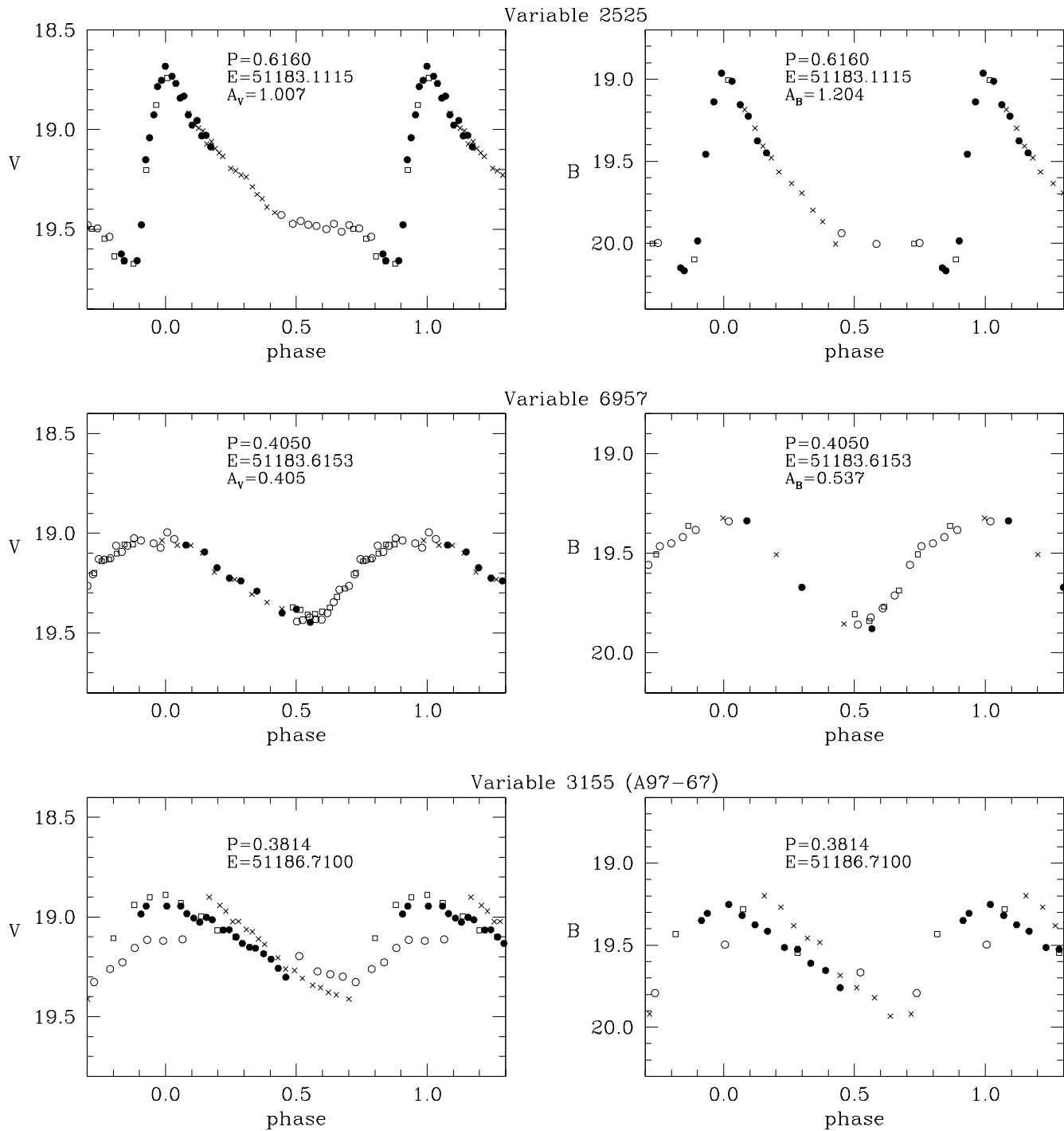


Fig. 8.— V and B light curves of RR Lyrae variables falling in our fields. From top to bottom an R Rab, an RRc and an RRd variable. Different symbols are used for data corresponding to different nights.

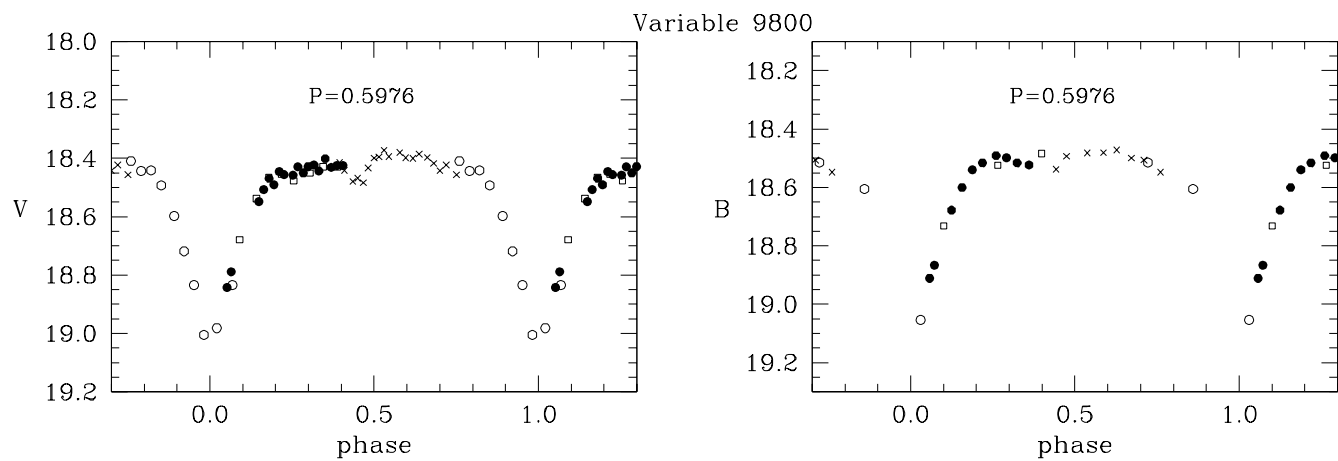


Fig. 9.— V and B light curves of an eclipsing binary falling in field A.

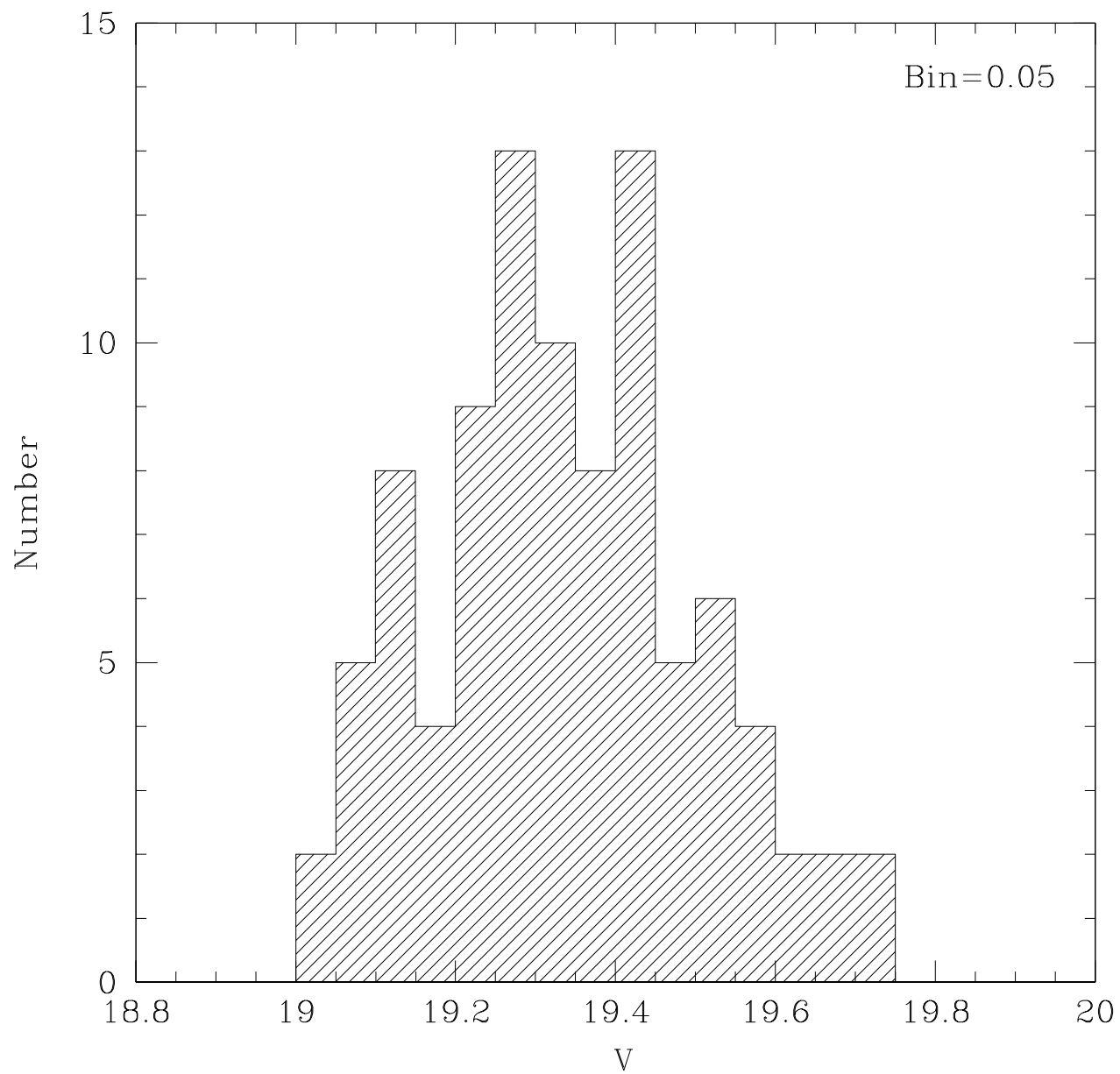


Fig. 10.— Number $vs \langle V \rangle$ histogram of the single-mode RR Lyrae variables with complete light curve (93 objects).

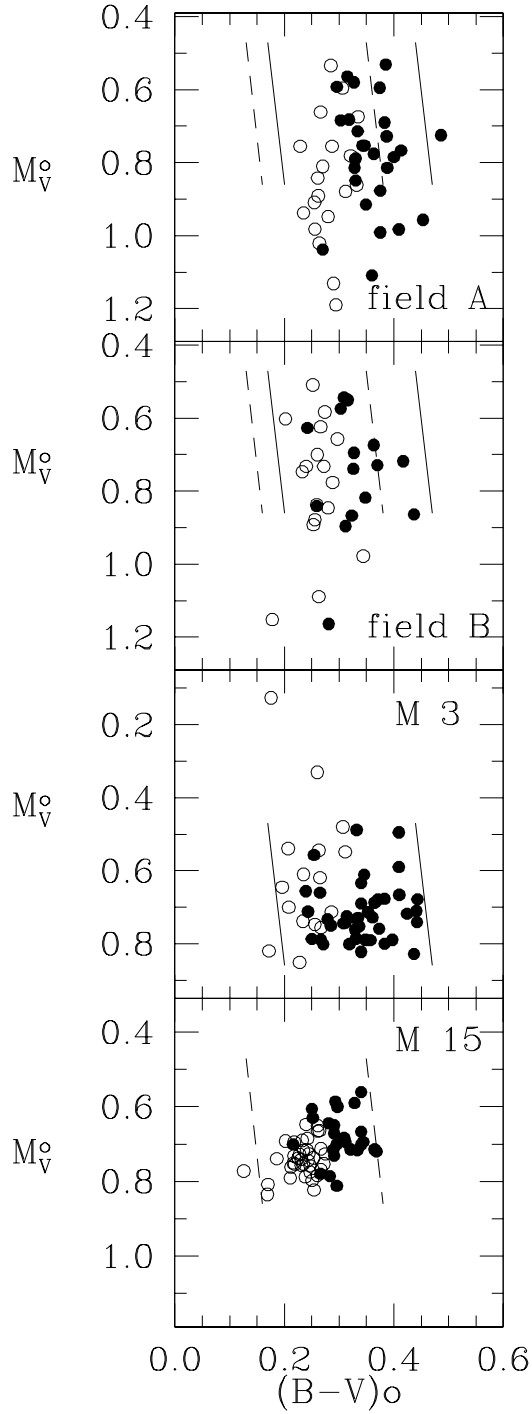


Fig. 11.— Comparison of the M_{V0} vs $(\langle B \rangle - \langle V \rangle)_0$ distributions of the LMC RR Lyrae's in field A and B separately, with the instability strips defined by the variables in the globular clusters M3 (Carretta et al. 1998) and M15 (Bingham et al. 1984), whose edges are given by the solid and dashed lines, respectively.

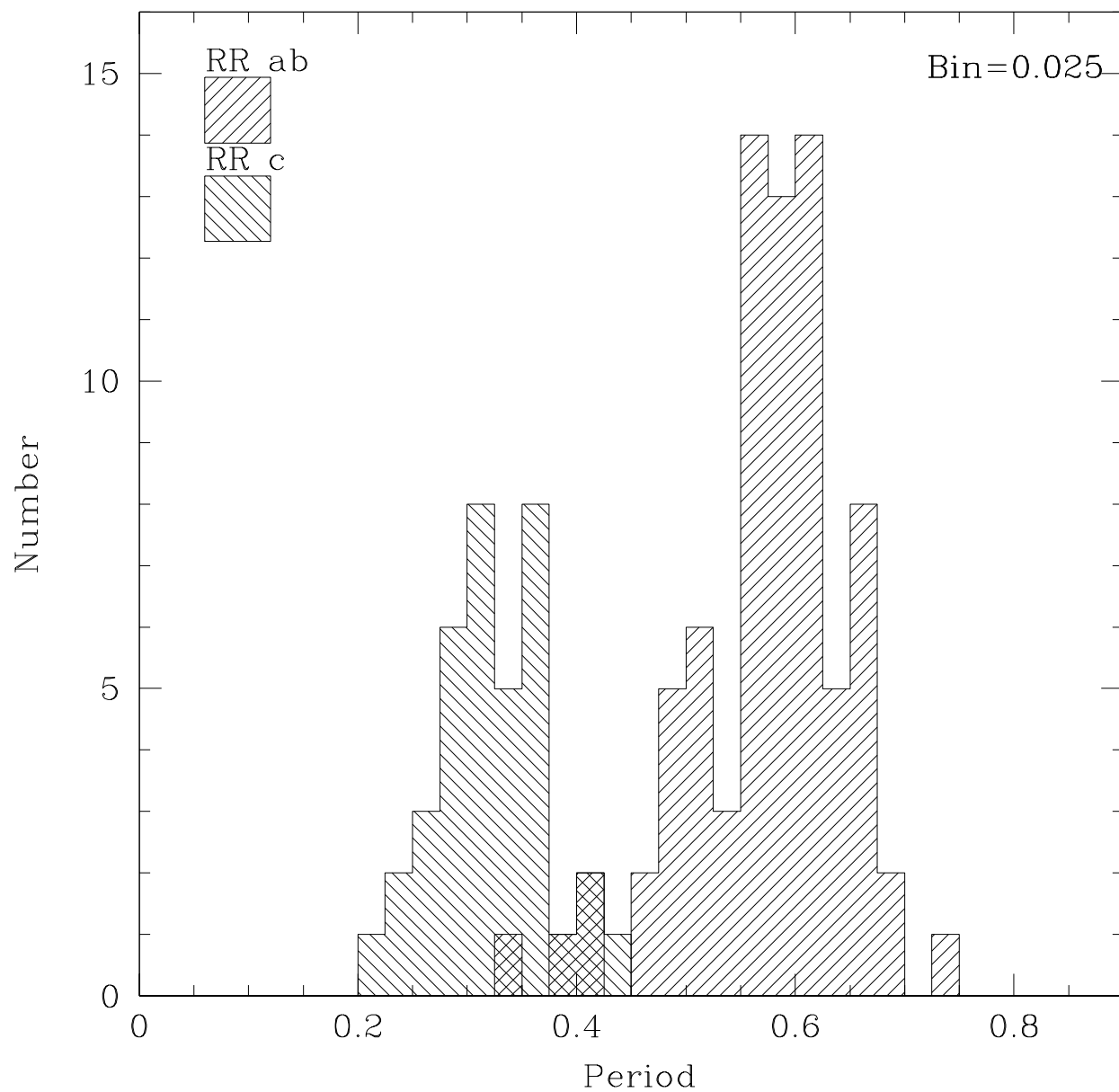


Fig. 12.— Number *vs* Period histogram of the single-mode RR Lyrae variables in our sample (115 objects).

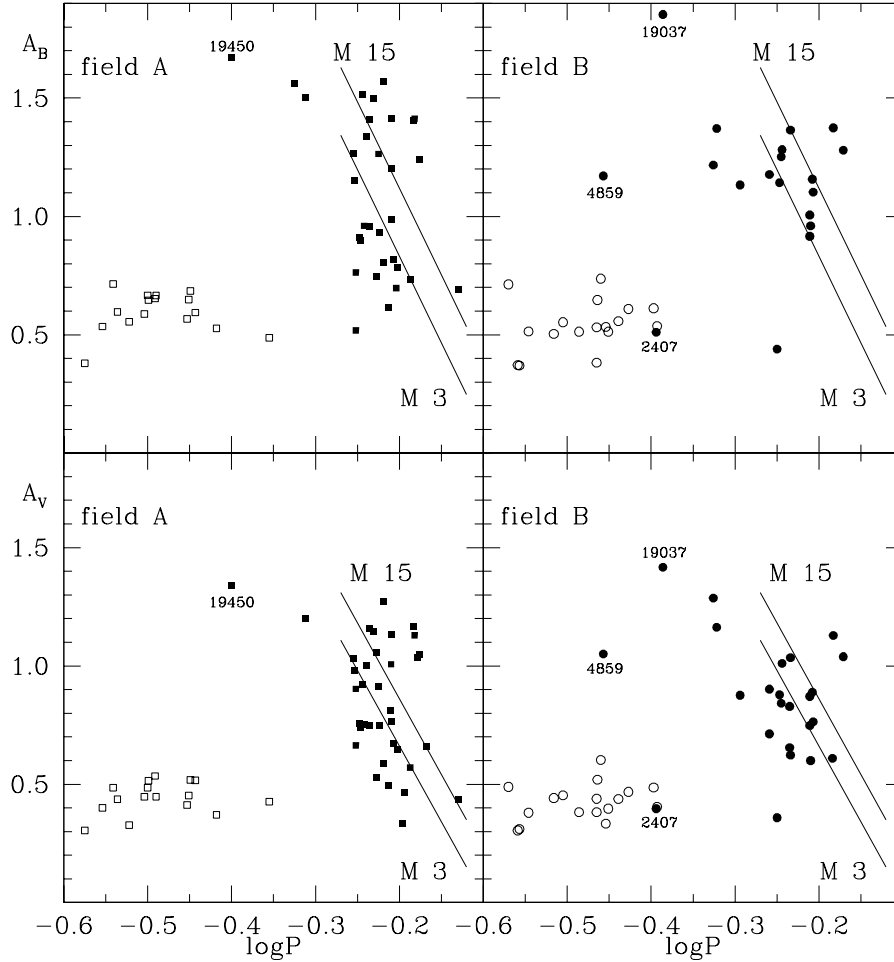


Fig. 13.— A_B vs $\log P$ and A_V vs $\log P$ diagrams for the RR Lyrae’s with complete B and V light curves in field A and B, separately. Solid lines show the distributions defined by the *ab* type RR Lyrae variables in the globular clusters M3 (Carretta et al. 1998) and M15 (Bingham et al. 1984) derived as described in Section 4.2. Different symbols refer to *ab* (filled circles) and *c* type (open circles) variables, respectively.

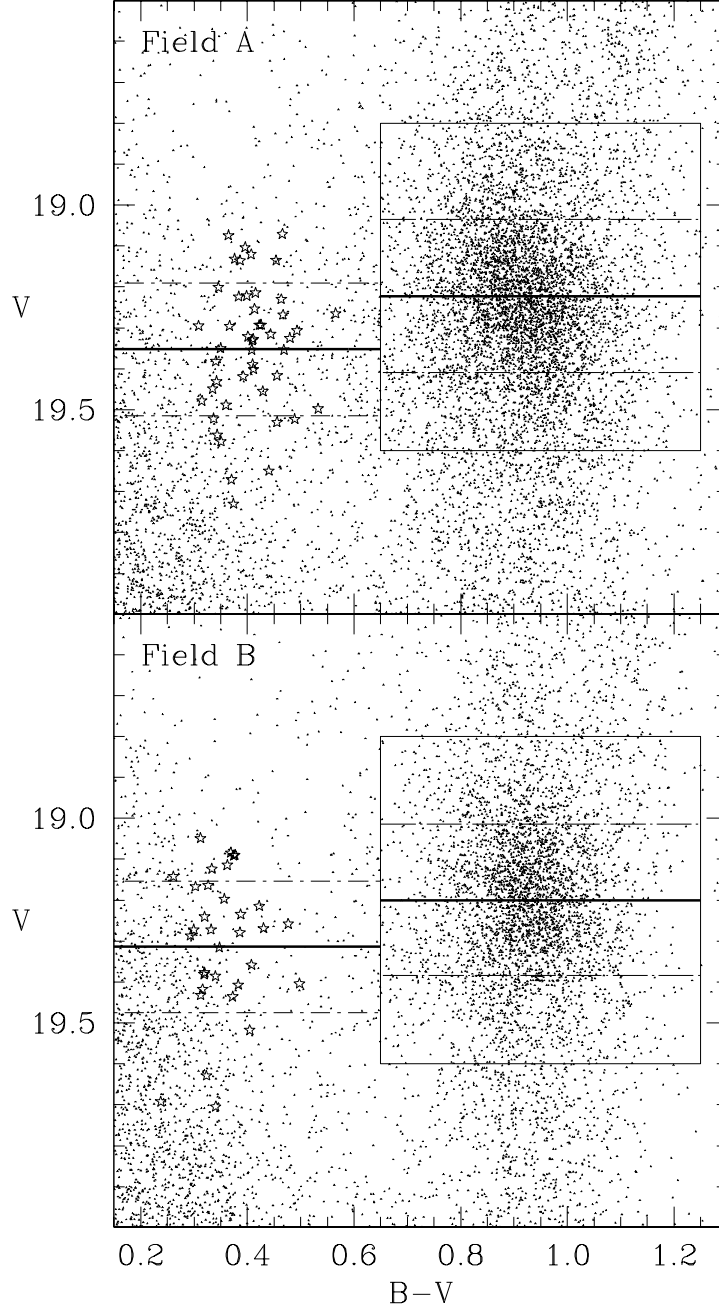


Fig. 14.— Enlargement of the regions containing the RR Lyrae and clump stars in the HR diagram of field A (top panel) and B (lower panel), respectively. Solid lines indicate the average levels of the RR Lyrae’s ($\langle V(\text{RR-A}) \rangle = 19.352$ mag, $\langle V(\text{RR-B}) \rangle = 19.314$ mag) and clump stars ($\langle V_{\text{Clump-A}} \rangle = 19.223$ mag, $\langle V_{\text{Clump-B}} \rangle = 19.200$ mag) in each field. Dotted-dashed lines represent the 1σ deviations from the averages (0.16 and 0.19 mag for RR Lyrae’s and clumps stars, respectively).